

Application number: H04-235534

Date of filing: September 3, 1992

Publication number: H06-28455

Date of publication of application: February 4, 1994

Applicant: DAINIPPON PRINTING CO LTD

Inventor: Ueda, Tomoaki

Title of the Invention: Tomogram image processing method, organism magnetic field measuring method, organism magnetic field-measured outcome display method, and apparatus therefore

[Scope of the Claim]

[Claim 1]

A tomogram image processing method, comprising the steps of:

- a) carrying out an interpolation operation on a plurality of tomogram images of a test boy sliced in an area at predetermined intervals to obtain stereoscopic image data elements;
- b) dividing said area into small stereoscopic segments;
- c) counting the number of said stereoscopic image data elements for each of said small stereoscopic segments; and
- d) binarizing said small stereoscopic segments on the basis of the number of said stereoscopic image data elements.

[Claim 2]

A tomogram image processing apparatus, comprising:

- interpolation carrying out means (3) for carrying out an interpolation operation on a plurality of tomogram images of a test boy sliced in an area at predetermined intervals to obtain stereoscopic image data elements;
- area dividing means (7) for dividing said area into small stereoscopic segments;
- stereoscopic image counting means (8) for counting the number of said stereoscopic image data elements for each of said small stereoscopic segments; and
- binarizing means (9, 10) for binarizing said small stereoscopic segments on the basis of the number of said stereoscopic image data elements.

[Claim 3]

An organism magnetic field measuring method, comprising the steps of:

- e) carrying out a plurality of Biot-Savart law calculations on a plurality of magnetic field information elements respectively for a plurality of vertexes of said small stereoscopic segments obtained in the tomogram image processing method as set forth in claim 1;
- f) adding up the results of the Biot-Savart law calculations to obtain a calculated magnetic field value;
- g) calculating a difference between said calculated magnetic field value and a measured magnetic field value;
- h) correcting data on said magnetic field sources included in the results of the

Biot-Savart law calculations in accordance with said difference;

- i) judging whether or not said difference is vanishingly small;
- j) repeating said step (e) through step (h) when it is judged in said step (i) that said difference is not vanishingly small; and

k) outputting, as an organism magnetic field-measured outcome, said data on said magnetic field sources included in the results of the Biot-Savart law calculations carried out in said step (h) when it is judged in said step (i) that said difference is vanishingly small.

[Claim 4]

An organism magnetic field measuring method as set forth in claim 4, in which

said step (h) is replaced with the steps of:

h1) calculating a difference between a coordinate of each of said vertexes of said small stereoscopic segments and a coordinate of each of corrected vertexes of said small stereoscopic segments;

h2) calculating said coordinate of each of said corrected vertexes of said small stereoscopic segments on the basis of a code of said difference calculated in said step (h1); and

h3) redistributing an estimate value of said magnetic field source in accordance with said difference calculated in said step (h1) for each of said corrected vertexes of said small stereoscopic segments calculated in said step (h2).

[Claim 5]

An organism magnetic field measuring apparatus, comprising:

calculating means (111, 112, ..., 11m; 101, 102, ..., 10m) for carrying out a plurality of Biot-Savart law calculations on a plurality of magnetic field information elements respectively for a plurality of vertexes of said small stereoscopic segments obtained in the tomogram image processing method as set forth in claim 1;

adding means (20; 200) for adding up the results of the Biot-Savart law calculations outputted from said calculating means (111, 112, ..., 11m; 101, 102, ..., 10m) to obtain a calculated magnetic field value;

error calculating means (30; 300) for calculating a difference between said calculated magnetic field value outputted from said adding means (20; 200) and a measured magnetic field value;

correcting means (111a, 112a, ..., 11ma) for correcting data on said magnetic field sources included the result of the Biot-Savart law calculations outputted from said calculating means (111, 112, ..., 11m; 101, 102, ..., 10m) in accordance with said difference; and

corrected result collecting means (40; 500) for collecting the results of the Biot-Savart law calculations corrected by said correcting means (111a, 112a, ..., 11ma) and outputting them therethrough as an organism magnetic field-measured outcome.

[Claim 6]

An organism magnetic field measuring apparatus as set forth in claim 5, further comprising:

as correcting means, difference calculating means (41i) for calculating a difference between a coordinate of each of said vertexes of said small stereoscopic segments and a coordinate of each of corrected vertexes of said small stereoscopic segments;

corrected vertex extracting means (42i) for calculating said coordinate of each of said corrected vertexes of said small stereoscopic segments on the basis of a code of said difference calculated by said difference calculating means (41i); and

redistributing means (43i, 44i, 45i) for redistributing an estimate value of said magnetic field source in accordance with said difference calculated by said difference calculating means (41i) for each of said corrected vertexes of said small stereoscopic segments calculated by said corrected vertex extracting means (42i).

7. An organism magnetic field-measured outcome display method of displaying an organism magnetic field-measured outcome along with an organism structure reference image, comprising the steps of:

l) calculating absolute values of said organism magnetic field-measured outcomes for a plurality of vivo points;

m) setting up a size of a reference graphic for each of said vivo points on the basis of said absolute values calculated in said step (l); and

n) displaying said reference graphic whose sizes is set up in said step (m) along with said organism structure reference image for each of said vivo points.

8. An organism magnetic field-measured outcome display method of displaying an organism magnetic field-measured outcome as set forth in claim 7, in which said reference graphic is in the form of a circular shape.

9. An organism magnetic field-measured outcome display apparatus for displaying organism magnetic field-measured outcomes along with an organism structure reference image, comprising:

reference graphic size calculating means (700) for calculating absolute values of said organism magnetic field-measured outcomes for a plurality of vivo points, and setting up a size of a reference graphic for each of said vivo points on the basis of said absolute values thus calculated;

organism structure displaying means (800) for displaying said organism structure reference image; and

reference graphic displaying means (900) for displaying said reference graphic whose size is set up by said reference graphic size calculating means (700) for each of said vivo points.

10. An organism magnetic field-measured outcome display apparatus as set forth in claim 9, in which said reference graphic is in the form of a circular shape.

[Detailed Explanation of the Invention]

[0001]

[Industrial Field in which the Invention is Used]

The present invention relates to a tomogram image processing method, an organism magnetic field measuring method, an organism magnetic field-measured outcome display method, and apparatuses for carrying out the respective methods, and

more particularly, to a tomogram image processing method of and apparatus for obtaining fine image data based on tomogram images sliced at respective predetermined intervals, an organism magnetic field measuring method of and apparatus for analyzing an organism magnetic field source based on fine image data provided by the tomogram image processing method, and an organism magnetic field-measured outcome display method of and apparatus for displaying the analyzed outcome of the organism magnetic field source in an easily recognizable condition.

[0002]

[Description of the Prior Art]

There have been provided a wide variety of conventional methods for visually superimposing magnetic field sources on tomogram images such as for example MRI images in order to display an organism magnetic field-measured outcome in an easily recognizable condition. As a method of visually superimposing magnetic field sources on tomogram images have been proposed a method of two-dimensionally displaying the magnetic field source under the condition that the magnetic field source is superimposed on the closest tomogram image and a method of three-dimensionally displaying the magnetic field source under the condition that the magnetic field source is superimposed on a plurality of tomogram images.

[0003]

As methods of measuring an organism magnetic field there have been proposed two methods consisting of a first measuring method and a second measuring method. The first measuring method is to be carried out under an assumption that the magnetic field source has a single dipole, and the second measuring method is to be carried out under an assumption that the magnetic field source has a plurality of current elements. The first measuring method comprises the step of calculating the position and the direction of the single dipole based on a plurality of outcomes of magnetic fields measurement measured at a plurality of points in the vicinity of a body surface. The second measurement method comprises the steps of measuring a magnetic field assuming that the magnetic field source has a predetermined number of current elements (usually 10 to 100); detecting points at which the measured magnetic field is remarkably greater than the predetermined number of current elements; and calculating the position and the direction of the current elements by performing a computation at the detected points.

[0004]

Furthermore, as methods of displaying an outcome of a measured organism magnetic field, there are publicly known an arrow mapping display method and a contour mapping display method. The arrow mapping display method comprises the steps of measuring an organism magnetic field, analyzing a magnetic field based on the measured organism magnetic field to obtain a plurality of current elements, and displaying the current elements thus obtained in the form of a current vector. The contour mapping display method comprises the steps of displaying the measured organism magnetic field in the form of an isomagnetic line. Furthermore, in order to carry out such display methods in a medical diagnoses, it is also proposed to display

arrows indicative of the current vectors or the isomagnetic lines superimposed on the MRI pictorial images so as to visually represent the current elements or the isomagnetic lines in internal organs.

[0005]

[Problem(s) to be Solved by the Invention]

In the case that the two-dimensional display method in the abovementioned magnetic field source display methods is adopted, there is an inconvenience that it becomes very difficult for a medical doctor to recognize the position of the magnetic field source even though the medical doctor would carefully observe a plurality of the tomogram images by the reason that the tomogram image having the magnetic field source superimposed thereon is scarcely displayed. Moreover, although the tomogram image having the magnetic field source superimposed thereon should be selected and displayed, it is quite difficult to detect the relative position of the magnetic field source based on the selected tomogram image.

[0006]

Further, in the case that the three-dimensional display method in the abovementioned magnetic field source display methods is adopted, there is another inconvenience that it is very difficult to recognize how the magnetic field source is inwardly deep and widespread by the reason that there are no marks indicating the magnetic field except for the tomogram images. Moreover, it is also difficult to detect the position of the magnetic field relative to the internal organs because there are provided only a few tomogram images having the magnetic field superimposed thereon. In the case that the aforementioned first measuring method to be carried out under an assumption that the magnetic field source has a single dipole is adopted, there is further another inconvenience that the measured outcome is apt to converge on an excessively profound solution in addition to being not capable of measuring a distributive magnetic field source to be represented by a volume current flowing in the internal organ in pulsation by the reason that a single dipole is only obtained as the measured outcome.

[0007]

In the case that the aforementioned second measuring method to be carried out under an assumption that the magnetic field source includes a plurality of current elements is adopted, it becomes possible to measure the distributive magnetic field source. However, the fact that around 30-100 elements of currents are generally provided leads to the fact that it is required to calculate an estimate of each of current elements based on a plurality of magnetic field measuring values after setting up around 200-1000 channels of an array sensor and obtaining the plurality of magnetic field measuring values in the case that all of the current elements are to be measured. There is an inconvenience that the processing load to calculate the estimate in the abovementioned case requires T. FLOPS so that the system itself becomes considerably large in scale and cost. There is another inconvenience that the estimate thus calculated converges on the local minima, thereby remarkably aggravating the accuracy of the estimate of each of the current elements.

[0008]

Any of the abovementioned arrow mapping display method and the contour mapping display method is appropriate for visually displaying the organism magnetic field-measured value in a particular timing, in other words, for visually displaying an organism magnetic field-measured distribution. This means that the both of the abovementioned arrow mapping display method and the contour mapping display method are inappropriate for displaying the organism magnetic field-measuring value of internal organs in pulsation. More particularly, although it is possible to dynamically display current elements by means of the arrow map display method, a large number of the current elements in the internal organs must be set up in order to display the volume current. Thus, a remarkably large number of the current elements must be displayed. Further, there is an inconvenience that it is difficult to recognize, for example, the propagation status of a visceral excitation current even though an MRI pictorial image and an arrow in an overlap display are carefully observed since the direction and dimension of each of the current elements change from hour to hour.

[0009]

The contour mapping display method cannot be adopted for continuously displaying the organism magnetic field-measured value by the reason that the isomagnetic line is unsuitable for displaying each of the current elements. This leads to the fact that the contour map display method cannot be carried out to visualize the propagation status of the visceral excitation current.

[0010]

[Purpose of the Invention]

In order to solve the abovementioned problems, it is therefore a first object of the present invention to provide a tomogram image processing method and apparatus capable of obtaining fine image data based on fine tomogram image data of such as internal organs sliced at respective predetermined intervals, it is therefore a second object of the present invention to provide an organism magnetic field measuring method and apparatus capable of analyzing an organism magnetic field source easily and precisely based on the fine tomogram image data obtained by the tomogram image processing method, and it is therefore a third object of the present invention to provide an organism physical quantity-measured outcome display method and apparatus capable of continuously displaying the organism physical quantity-measured value in an easily recognizable condition.

[0011]

[Measures to Solve the Problems]

In order to achieve the abovementioned first object, there is provided a tomogram image processing method as set forth in claim 1, comprising the steps of: a) carrying out an interpolation operation on a plurality of tomogram images of a test boy sliced in an area at predetermined intervals to obtain stereoscopic image data elements; b) dividing said area into small stereoscopic segments; c) counting the number of said stereoscopic image data elements for each of said small stereoscopic segments; and d) binarizing said small stereoscopic segments on the basis of the number of said

stereoscopic image data elements.

[0012]

A tomogram image processing apparatus as set forth in claim 2, comprises: interpolation carrying out means (3) for carrying out an interpolation operation on a plurality of tomogram images of a test boy sliced in an area at predetermined intervals to obtain stereoscopic image data elements; area dividing means (7) for dividing said area into small stereoscopic segments; stereoscopic image counting means (8) for counting the number of said stereoscopic image data elements for each of said small stereoscopic segments; and binarizing means (9, 10) for binarizing said small stereoscopic segments on the basis of the number of said stereoscopic image data elements.

[0013]

In order to achieve the foregoing second object, there is provided an organism magnetic field measuring method as set forth in claim 3, comprising the steps of: e) carrying out a plurality of Biot-Savart law calculations on a plurality of magnetic field information elements respectively for a plurality of vertexes of said small stereoscopic segments obtained in the tomogram image processing method as set forth in claim 1; f) adding up the results of the Biot-Savart law calculations to obtain a calculated magnetic field value; g) calculating a difference between said calculated magnetic field value and a measured magnetic field value; h) correcting data on said magnetic field sources included in the results of the Biot-Savart law calculations in accordance with said difference; i) judging whether or not said difference is vanishingly small; j) repeating said step (e) through step (h) when it is judged in said step (i) that said difference is not vanishingly small; and k) outputting, as an organism magnetic field-measured outcome, said data on said magnetic field sources included in the results of the Biot-Savart law calculations carried out in said step (h) when it is judged in said step (i) that said difference is vanishingly small.

[0014]

In an organism magnetic field measuring method as set forth in claim 4, said step (h) is replaced with the steps of: h1) calculating a difference between a coordinate of each of said vertexes of said small stereoscopic segments and a coordinate of each of corrected vertexes of said small stereoscopic segments; h2) calculating said coordinate of each of said corrected vertexes of said small stereoscopic segments on the basis of a code of said difference calculated in said step (h1); and h3) redistributing an estimate value of said magnetic field source in accordance with said difference calculated in said step (h1) for each of said corrected vertexes of said small stereoscopic segments calculated in said step (h2).

[0015]

An organism magnetic field measuring apparatus as set forth in claim 5, comprises: calculating means (111, 112,, 11m; 101, 102,, 10m) for carrying out a plurality of Biot-Savart law calculations on a plurality of magnetic field information elements respectively for a plurality of vertexes of said small stereoscopic segments obtained in the tomogram image processing method as set forth in claim 1; adding

means (20; 200) for adding up the results of the Biot-Savart law calculations outputted from said calculating means (111, 112, ..., 11m; 101, 102, ..., 10m) to obtain a calculated magnetic field value; error calculating means (30; 300) for calculating a difference between said calculated magnetic field value outputted from said adding means (20; 200) and a measured magnetic field value; correcting means (111a, 112a, ..., 11ma) for correcting data on said magnetic field sources included the result of the Biot-Savart law calculations outputted from said calculating means (111, 112, ..., 11m; 101, 102, ..., 10m) in accordance with said difference; and corrected result collecting means (40; 500) for collecting the results of the Biot-Savart law calculations corrected by said correcting means (111a, 112a, ..., 11ma) and outputting them therethrough as an organism magnetic field-measured outcome.

[0016]

An organism magnetic field measuring apparatus as set forth in claim 6, further comprises: .as correcting means, difference calculating means (41i) for calculating a difference between a coordinate of each of said vertexes of said small stereoscopic segments and a coordinate of each of corrected vertexes of said small stereoscopic segments; corrected vertex extracting means (42i) for calculating said coordinate of each of said corrected vertexes of said small stereoscopic segments on the basis of a code of said difference calculated by said difference calculating means (41i); and redistributing means (43i, 44i, 45i) for redistributing an estimate value of said magnetic field source in accordance with said difference calculated by said difference calculating means (41i) for each of said corrected vertexes of said small stereoscopic segments calculated by said corrected vertex extracting means (42i).

[0017]

In order to achieve the foregoing third object, there is provided a method as set forth in claim 7 of displaying an organism magnetic field-measured outcome along with an organism structure reference image, comprising the steps of: l) calculating absolute values of said organism magnetic field-measured outcomes for a plurality of vivo points; m) setting up a size of a reference graphic for each of said vivo points on the basis of said absolute values calculated in said step (l); and n) displaying said reference graphic whose sizes is set up in said step (m) along with said organism structure reference image for each of said vivo points. In a method of displaying an organism magnetic field-measured outcome as set forth in claim 8, said reference graphic is in the form of a circular shape.

[0018]

An organism magnetic field-measured outcome display apparatus as set forth in claim 9 for displaying organism magnetic field-measured outcomes along with an organism structure reference image, comprises: reference graphic size calculating means (700) for calculating absolute values of said organism magnetic field-measured outcomes for a plurality of vivo points, and setting up a size of a reference graphic for each of said vivo points on the basis of said absolute values thus calculated; organism structure displaying means (800) for displaying said organism structure reference image; and reference graphic displaying means (900) for displaying said reference

graphic whose size is set up by said reference graphic size calculating means (700) for each of said vivo points. In an organism magnetic field-measured outcome display apparatus as set forth in claim 10, said reference graphic is in the form of a circular shape.

[0019]

[Function]

A tomogram image processing method as set forth in claim 1, comprising the steps of: a) carrying out an interpolation operation on a plurality of tomogram images of a test boy sliced in an area at predetermined intervals to obtain stereoscopic image data elements; b) dividing said area into small stereoscopic segments; c) counting the number of said stereoscopic image data elements for each of said small stereoscopic segments; and d) binarizing said small stereoscopic segments on the basis of the number of said stereoscopic image data elements, can obtain the stereoscopic image data elements corresponding to all of the small stereoscopic segments by carrying out the interpolation operation on a plurality of tomogram images of the test body even through some tomogram images sliced at the intervals should fail to be provided. Further, the tomogram image processing method thus constructed can obtain a simplified stereoscopic image by the reason that the small stereoscopic segments are binarized on the basis of the number of the stereoscopic image data elements. This leads to the fact that the stereoscopic image obtained and displayed by the tomogram image processing method as set forth in claim 1 makes it possible for an operator to easily distinguish an area and/or a stereoscopic segment where an internal organ or the like is placed.

[0020]

Any of a linear interpolation arithmetical calculation, a spline interpolation arithmetical calculation, and the like may be appropriately selected and adopted for the abovementioned interpolation arithmetical operation. Further, an appropriate threshold value may be set up in order to adapt the numbers of the stereoscopic image data elements to be binarized to the numbers of the variety of the tomogram images and to the numbers of the internal organs to be processed. As a small stereoscopic segment, it is desirable to use a solid segment with which the segment can be filled densely. It more preferable to use a cube segment in order to simplify the treatments later performed.

[0021]

A tomogram image processing apparatus as set forth in claim 2, comprises: interpolation carrying out means (3) for carrying out an interpolation operation on a plurality of tomogram images of a test boy sliced in an area at predetermined intervals to obtain stereoscopic image data elements; area dividing means (7) for dividing said area into small stereoscopic segments; stereoscopic image counting means (8) for counting the number of said stereoscopic image data elements for each of said small stereoscopic segments; and binarizing means (9, 10) for binarizing said small stereoscopic segments on the basis of the number of said stereoscopic image data elements. The stereoscopic image obtained and displayed by the tomogram image

processing apparatus thus constructed makes it possible for an operator to easily distinguish an area and/or a stereoscopic segment where an internal organ or the like is placed. The organism magnetic field measuring method as set forth in claim 3, comprising the steps of: e) carrying out a plurality of Biot-Savart law calculations on a plurality of magnetic field information elements respectively for a plurality of vertexes of said small stereoscopic segments obtained in the tomogram image processing method as set forth in claim 1; f) adding up the results of the Biot-Savart law calculations to obtain a calculated magnetic field value; g) calculating a difference between said calculated magnetic field value and a measured magnetic field value; h) correcting data on said magnetic field sources included in the results of the Biot-Savart law calculations in accordance with said difference; i) judging whether or not said difference is vanishingly small; j) repeating said step (e) through step (h) when it is judged in said step (i) that said difference is not vanishingly small; and k) outputting, as an organism magnetic field-measured outcome, said data on said magnetic field sources included in the results of the Biot-Savart law calculations carried out in said step (h) when it is judged in said step (i) that said difference is vanishingly small, can obtain the data on the magnetic field source for each of a plurality of vertexes of said small stereoscopic segments by the reason that data on said magnetic field sources included in the results of the Biot-Savart law calculations is corrected until the difference between said calculated magnetic field value and a measured magnetic field value becomes vanishingly small. Furthermore, the number of unknown factors to be estimated can be largely reduced by the reason that the position of each of the vertexes of the small stereoscopic segments is known.

[0022]

The organism magnetic field measuring method as set forth in claim 4, in which said step (h) is replaced with the steps of: h1) calculating a difference between a coordinate of each of said vertexes of said small stereoscopic segments and a coordinate of each of corrected vertexes of said small stereoscopic segments; h2) calculating said coordinate of each of said corrected vertexes of said small stereoscopic segments on the basis of a code of said difference calculated in said step (h1); and h3) redistributing an estimate value of said magnetic field source in accordance with said difference calculated in said step (h1) for each of said corrected vertexes of said small stereoscopic segments calculated in said step (h2), can obtain accurate information on the magnetic field source by the reason that even magnetic field source vectors assigned in positions adjoining to each other, equal to each other in magnitude but opposing to each other in direction can be calibrated.

[0023]

In the organism magnetic field measuring apparatus as set forth in claim 5, the calculating means is operative to carry out a plurality of Biot-Savart law calculations on a plurality of magnetic field information elements respectively for a plurality of vertexes of said small stereoscopic segments obtained in the tomogram image processing method as set forth in claim 1, and the adding means is operative to add up the results of the Biot-Savart law calculations outputted from said calculating means to

obtain a calculated magnetic field value. The error calculating means is operative to calculate a difference between said calculated magnetic field value outputted from said adding means and a measured magnetic field value, and the correcting means is operative to correct data on said magnetic field sources included the result of the Biot-Savart law calculations outputted from said calculating means in accordance with said difference. After the correcting means has corrected the data on the magnetic field sources, the corrected result collecting means is operative to collect the results of the Biot-Savart law calculations thus corrected output them therethrough as an organism magnetic field-measured outcome. The organism magnetic field measuring apparatus thus constructed makes it possible for an operator to obtain the data on the magnetic field source for each of the vertexes of the small stereoscopic segments. Furthermore, the number of unknown factors to be estimated can be largely reduced by the reason that the position of each of the vertexes of the small stereoscopic segments is known.

[0024]

An organism magnetic field measuring apparatus as set forth in claim 6, further comprises: ,as correcting means, difference calculating means (41i) for calculating a difference between a coordinate of each of said vertexes of said small stereoscopic segments and a coordinate of each of corrected vertexes of said small stereoscopic segments; corrected vertex extracting means (42i) for calculating said coordinate of each of said corrected vertexes of said small stereoscopic segments on the basis of a code of said difference calculated by said difference calculating means (41i); and redistributing means (43i, 44i, 45i) for redistributing an estimate value of said magnetic field source in accordance with said difference calculated by said difference calculating means (41i) for each of said corrected vertexes of said small stereoscopic segments calculated by said corrected vertex extracting means (42i), can obtain accurate information on the magnetic field source by the reason that even magnetic field source vectors assigned in positions adjoining to each other, equal to each other in magnitude but opposing to each other in direction can be calibrated.

[0025]

The organism magnetic field measuring method will be described in detail hereinlater. As a result of enormous researches made by the inventor of the present invention in the field of measuring the organism magnetic field, it is found out that the position of each of the vertexes of the small stereoscopic segments is known because of the fact that each of the vertexes of the small stereoscopic segments has been obtained by the tomogram image processing method. This leads to the fact that information required to obtain the information on the magnetic field source is a vector component of the current element only.

[0026]

Even if the number of the small stereoscopic segments increases, the number of the vertexes does not increase in proportion to the increased number of the small stereoscopic segments by the reason that one vertex of one small stereoscopic segment serves as the vertex of the adjacent small stereoscopic segment. In the case that the

number of the small stereoscopic segments is large enough, the number of the vertexes and the number of the small stereoscopic segments are approximately equal to each other. By the fact that a current element of one vertex is related to that of an adjacent vertex, the amount of data of the current element of one vertex can be reduced remarkably, compared to the case that a general unknown quantity is estimated.

[0027]

The number of current elements to be finally estimated is remarkably small by the reason that the current element of a vertex having no magnetic field source converges on a zero vector. The inventions defined in claims 3 through 6 are made based on the abovementioned knowledge. A predetermined number of the magnetic field measuring values are obtained based on the efficiency and the capacity of the measuring system without considering an unknown number of current elements when the unknown current elements [the number is unknown either] are estimated at the start of measuring. A precise estimate of the unknown current elements can be achieved by repeating the correcting process of the data of the magnetic field source based on the predetermined number of the magnetic field measuring values, and the estimate outcome of which can be adopted as an organism magnetic field measured outcome.

[0028]

The organism magnetic field-measured outcome display method as set forth in claim 7 of displaying an organism magnetic field-measured outcome along with an organism structure reference image, comprising the steps of: l) calculating absolute values of said organism magnetic field-measured outcomes for a plurality of vivo points; m) setting up a size of a reference graphic for each of said vivo points on the basis of said absolute values calculated in said step (l); and n) displaying said reference graphic whose sizes is set up in said step (m) along with said organism structure reference image for each of said vivo points, makes it possible for an operator to recognize, for example, the distributed condition of the maximal organism magnetic field-measured outcome in comparison with the case that the magnetic field measured outcome is displayed with the direction and the length of the arrows. The direction components of the organism magnetic field cannot be recognized. It is, however, not inconvenient by the reason that the organism magnetic field measured outcome can be dynamically displayed, thereby making it possible for an operator to easily recognize, for example, the time-variant fluctuation of the distributed condition of the maximal organism magnetic field measured outcome. The organism magnetic field-measured outcome display method thus constructed can satisfy the requirement of the medical analysis that the distribution of the maximal organism magnetic field-measured outcome and the time-variant fluctuation should be represented in an easily understandable manner. This leads to the fact that the organism magnetic field-measured outcome display method thus constructed is most appropriate for the medical analysis.

[0029]

In the organism magnetic field-measured outcome display method as set forth in claim 8, said reference graphic is in the form of a circular shape. In addition to the

operations as set forth in claim 7 the magnetic field-measured outcome display method as set forth in claim 8 can considerably enlarge a clearance between the reference graphics, thereby making it possible for an operator to recognize the organism structure reference image as a background. The organism magnetic field-measured outcome display apparatus as set forth in claim 9 is operative to display organism magnetic field-measured outcomes along with an organism structure reference image in a manner that the reference graphic size calculating means is operative to calculate the absolute values of said organism magnetic field-measured outcomes for a plurality of vivo points, and setting up a size of a reference graphic for each of said vivo points on the basis of said absolute values thus calculated, the organism structure displaying means is operative to display said organism structure reference image; and the reference graphic displaying means is operative to display said reference graphic whose size is set up by said reference graphic size calculating means for each of said vivo points. The organism magnetic field-measured outcome display apparatus thus constructed makes it possible for an operator to recognize, for example, the distributed condition of the maximal organism magnetic field-measured outcome in comparison with the case that the magnetic field measured outcome is displayed with the direction and the length of the arrows. The direction components of the organism magnetic field cannot be recognized. It is, however, not inconvenient by the reason that the organism magnetic field measured outcome can be dynamically displayed, thereby making it possible for an operator to easily recognize, for example, the time-variant fluctuation of the distributed condition of the maximal organism magnetic field measured outcome. The organism magnetic field-measured outcome display apparatus thus constructed can satisfy the requirement of the medical analysis that the distribution of the maximal organism magnetic field-measured outcome and the time-variant fluctuation should be represented in an easily understandable manner. This leads to the fact that the organism magnetic field-measured outcome display apparatus thus constructed is most appropriate for the medical analysis.

[0030]

In the organism magnetic field-measured outcome display apparatus as set forth in claim 10, said reference graphic is in the form of a circular shape. In addition to the operations as set forth in claim 9 the magnetic field-measured outcome display apparatus as set forth in claim 10 can considerably enlarge a clearance between reference graphics, thereby making it possible for an operator to recognize the organism structure reference image as a background.

[0031]

[EMBODIMENT OF THE PRESENT INVENTION]

Preferred embodiments of the tomogram image processing method, the organism magnetic field measuring method, the organism magnetic field-measured outcome display method, and the apparatuses for the respective methods according to the present invention will now be described in detail in accordance with accompanying drawings. Referring now to the drawings, in particular to FIG. 1 of a flowchart, there is shown a preferred embodiment of the tomogram image processing method according

to the present invention. The tomogram image processing method comprises the steps of: waiting for receiving a plurality of tomogram images of a test boy sliced in an area at predetermined intervals (step SP 1); carrying out an interpolation operation on the plurality of received tomogram images to obtain interpolated tomogram images (step SP2); quantizing the received tomogram images and the interpolated tomogram images to obtain a plurality of squares each having a predetermined size (step SP3); dividing the area into a plurality of small stereoscopic segments each in the form of a cube shape having a center axis passing through the center of and a side equal in length to the side of the square (step SP4); counting the number of pixels constituting the received tomogram images and the interpolated tomogram images for each of the small stereoscopic segments (step SP5); judging whether or not the counted number is larger than a predetermined threshold value (for example, the average of all of the averages) for each of the small stereoscopic segments (step SP6), assigning each of the small stereoscopic segments, for which the counted number is judged in the step of SP6 to be larger than the threshold value, to "a small stereoscopic segment group to be displayed" (step SP7), and assigning each of the small stereoscopic segments, for which the counted number is judged in the step of SP7 to be not larger than the threshold value, to "a small stereoscopic segment group to be not displayed" (step SP8). The tomogram image processing method further comprises the steps of judging whether or not the step SP7 or the step SP8 has been performed for all of the small stereoscopic segments (step SP9). When it is judged in the step of SP9 that the step SP7 or the step SP8 has not been performed for a small stereoscopic segment, the step SP9 goes forward to the step SP10, in which the small stereoscopic segment is selected, and the step SP10 goes back to the step SP5. When it is judged in the step of SP9 that the step SP7 or the step SP8 has been performed for all of the small stereoscopic segment, the step SP9 goes forward to the step SP11, in which each of the small stereoscopic segments assigned to the small stereoscopic segment group to be displayed is visually displayed.

[0032]

It is needless to mention to the ratio of the number of pixels constituting the tomogram images to the number of pixels contained in a small stereoscopic segment for each of the small stereoscopic segments and a corresponding threshold value can be adopted in place of the number of pixels contained for each of the small stereoscopic segments. The present embodiment of the tomogram image processing method will be described in detail with reference to the drawings, in particular to FIGS. 2 through 4. FIG. 2 is a schematic diagram showing an example of a tomogram image, wherein the parts that are painted out indicates an internal organ of a human body. The tomogram image shown in FIG. 2 is constituted by a plurality of squares. As shown in FIG. 2, the center of each of the squares is shown with a small dot. This leads to the fact that a plurality of small stereoscopic segments each in the form of a cube shape having a center axis passing through the center of the square shown by the dot can be determined. As shown in FIG. 3, the small stereoscopic segments each having the number of pixels larger than a predetermined threshold value are assigned to the "small

stereoscopic segment group to be displayed" and the small stereoscopic segments each having the number of pixels not larger than a predetermined threshold value are assigned to the "small stereoscopic segment group to be not displayed". FIG. 4 is a perspective view corresponding to FIG. 3, and only the small stereoscopic segments assigned to the "small stereoscopic segment group to be displayed" is displayed. As will be seen in FIG. 4, the displayed small stereoscopic segments make it possible for an operator to visually recognize an internal organ.

[0033]

As will be understood from the foregoing description, carrying out a series of above-mentioned processes on all of the received tomogram images and the interpolated tomogram images makes it possible to visually display the organism internal organs as a solid model. It is, however, desirable to semi-transparently display the small stereoscopic segments assigned to the "small stereoscopic segment group to be displayed" so that the magnetic field source analyzing outcome can be easily recognized when a magnetic field source analyzing outcome is superimposed and displayed. Furthermore, specifying respective internal organs contained in the tomogram images makes it possible to display only the internal organs to be inspected or to display a plurality of the internal organs with their own colors. When an organism magnetic field source or the like, which will be described later, is analyzed, the tomogram image processing method according to the present invention thus constructed can process only the small stereoscopic segments assigned to the "small stereoscopic segment group to be displayed", thereby largely reducing arithmetical calculations required for the post processing by the reason that the small stereoscopic segments assigned to the "small stereoscopic segment group to be not displayed" correspond to a visceral cavity or the like and are accordingly ignored.

[0034]

[Second Embodiment]

Referring to the drawings, in particular to FIG. 5 of a block diagram, there is shown a second embodiment of the tomogram image processing apparatus according to the present invention. The tomogram image processing apparatus, comprises: a tomogram image storing unit 1 for storing therein a plurality of tomogram images, a first tomogram image selecting unit 2 for selecting a tomogram image to be processed among the tomogram images stored in the tomogram image storing unit 1, an interpolation carrying out unit 3 for carrying out an interpolation operation on the basis of the tomogram images selected by the first tomogram image selecting unit 2 to obtain interpolated tomogram images, an interpolation tomogram image storing unit 4 for storing the interpolated tomogram images obtained by the interpolation carrying out unit 3, a first repeat control unit 5 for having the tomogram image selecting unit 2 and the tomogram image interpolating unit 3 repeatedly operate for a necessary number of times, a second tomogram image selecting unit 6 for sequentially selecting a tomogram image from among the tomogram images stored in the tomogram image storing unit 1 or the interpolation tomogram image storing unit 4 in response to an end signal indicative of the end of the repeat control operation of the first repeat control unit 5, a

stereoscopic segment assigning unit 7 for assigning the tomogram image selected by the second tomogram image selecting unit 6 to a stereoscopic segment, a pixel number counting unit 8 for counting the number of pixels present in the stereoscopic segment, a judging unit 9 for judging whether or not the number of pixels counted by the pixel number counting unit 8 is larger than a predetermined threshold value, a display-stereoscopic segment assigning unit 10 for assigning the small stereoscopic segment, for which the counted number is judged by the judging unit 8 to be larger than the threshold value, to “a small stereoscopic segment group to be displayed”, a non-display-stereoscopic segment assigning unit 11 for assigning the small stereoscopic segment, for which the counted number is judged by the judging unit 8 to be not larger than the threshold value, to “a small stereoscopic segment group to be not displayed”, an assigning outcome storing unit 12 for storing therein the received tomogram images and the interpolated tomogram images in association with the small stereoscopic segments assigned to the respective small stereoscopic segment groups, a second repeat control unit 13 for controlling the second tomogram image selecting unit 6, the stereoscopic segment assigning unit 7, the pixel counting unit 8, the judging unit 9, the display-stereoscopic segment assigning unit 10 and the non-displaying assigning unit 11 to have the second tomogram image selecting unit 6, the stereoscopic segment assigning unit 7, the pixel counting unit 8, the judging unit 9, the display-stereoscopic segment assigning unit 10 and the non-displaying assigning unit 11 repeatedly operate for a necessary number of times, and a stereoscopic segment displaying unit 14 for visually displaying only the small stereoscopic segments assigned to the “small stereoscopic segment group to be displayed” in response to an end signal indicative of the end of the repeat control operation of the second repeat control unit 13.

[0035]

As will be seen from the foregoing description, it is to be understood that the tomogram processing apparatus according to the present invention thus constructed as shown in FIG. 5 can perform processing on the tomogram images as shown in FIGS. 2 through 4, and thus visually display only the small stereoscopic segments assigned to the “small stereoscopic segment group to be displayed”.

[0036]

[Third Embodiment]

Referring to the drawings, in particular to FIG. 6 of a block diagram, there is shown a third preferred embodiment of the organism magnetic field measuring apparatus according to the present invention. The organism magnetic field measuring apparatus is shown in FIG. 6 as comprising: a plurality of Biot-Savart arithmetical calculating units 111, 112, ..., 11m each for carrying out a Biot-Savart law calculation on a magnetic field information element for a vertex of the small stereoscopic segment obtained in the tomogram image processing method shown in FIG. 1 or the tomogram image processing apparatus shown in FIG. 5, an adding unit 20 for adding up the results of the Biot-Savart law calculations outputted from the Biot-Savart arithmetical calculating unit 111, 112, ..., 11m; 101, 102, ..., an error calculator 30 for calculating a difference between an added-up value Oj(t) outputted from the adding unit 20 and a

magnetic field-measured value $Sj(t)$ inputted as a teacher pattern, a plurality of correcting units 111a, 112a, ..., 11ma respectively for correcting vector components of current elements estimated by the Biot-Savart arithmetical calculating units 111, 112, ..., 11m based on the difference calculated by the error calculator 30, and a data collecting unit 40 for collecting the vector components of the current elements estimated by the Biot-Savart arithmetical calculating units 111, 112, ..., 11m and to output the vector components thus collected as an analyzing outcome. Furthermore, each of the Biot-Savart arithmetical calculating units 111, 112, ..., 11m is adapted to carry out a Biot-Savart law calculation on a magnetic field information element for a vertex of the small stereoscopic segment obtained at time "t" in the tomogram image processing method shown in FIG. 1 or by the tomogram image processing apparatus shown in FIG. 5, and correct the vector components of the estimated current elements in response to the difference $dj(t) = \{Sj(t) - Oj(t)\}$ calculated by the error calculator 30. The operations of the Biot-Savart arithmetical calculating units 111, 112, ..., 11m may be performed synchronously or asynchronously.

[0037]

The operation of the organism magnetic field measuring apparatus thus constructed will be described hereinlater. Magnetic field $Oj(t)$ to be analyzed is represented by the linear sum of the time "i", three-dimensional coordinate values xi , yi , zi ("i" is intended to mean a positive integer) of each vertex of the respective small stereoscopic segments, and functions gi (each of the functions is determined based on the Biot-Savart law). Each of the functions gi has vector components Pxi , Pyi , Pzi of the current elements. When only vector components on a plane are used as measurable components for a magnetic field sensor, any of the vector components can be omitted by applying the coordinates to the sensor. All of the three-dimensional coordinate values are known by the fact that the respective small stereoscopic segments are provided by the tomogram image processing method of FIG. 1 or the tomogram processing apparatus of FIG. 5.

[0038]

Accordingly, the organism magnetic field measuring apparatus thus constructed can obtain the added-up value $Oj(t)$ with the processes of: supplying "m" unit of the Biot-Savart arithmetical calculating units 111, 112, ..., 11m with the time "t" and the three-dimensional coordinate values of each of the vertexes of the respective small stereoscopic segments; performing the arithmetical calculation $g1$, $g2$, ..., gm respectively to calculate the function values, and supplying the adding unit 20 with all of the calculated values. The added-up value $O j (t)$ provided on the first iteration of the above-mentioned processes is however different from the actual measured value $S j (t)$ by the reason that the vector components of the respective current elements are set up at arbitrary numbers on the first iteration. The error calculator 30 is then operated to calculate a difference between actual measured value $Sj(t)$ and the added-up value $O j (t)$, and feed the difference thus calculated as an estimated error $dj (t)$ back to the respective correcting units 111a, 112a, ..., 11ma so that the Biot-Savart arithmetical calculating units 111, 112, ..., 11m will alter the

vector components of the respective Biot-Savart arithmetical calculating units until the estimated error $d_j(t)$ becomes small.

[0039]

The above-mentioned processes are repeated until the estimated error $d_j(t)$ becomes approximately zero. The data collecting unit 40 is then operated to collect the vector components of the current elements estimated by the Biot-Savart arithmetical calculating units 111, 112, ..., 11m and to output the vector components thus collected as an analyzing outcome. The vector component of the current element in each of the vertexes of the respective small stereoscopic segments can be outputted from the data collecting unit 40 at this stage. Further, an estimated error evaluating function $E_j(t)$ is defined by the formula: $E_j(t) = (1/2) \{S_j(t) - O_j(t)\}^2$, Equation 1 is obtained as follows.

[Equation 1]

$$\partial E_j(t) / \partial O_j(t) = -\{S_j(t) - O_j(t)\}$$

[0041]

If the vector component estimated by each of the Biot-Savart arithmetical calculating units is corrected based on a steepest descent method, the vector component, which minimizes the value of the estimated error evaluating function, can be obtained in accordance with the following Equation 2. Here, ϵ_k is a learning gain (a correcting gain) of the vector component a_{ik} .

[0042]

[Equation 2]

$$\begin{aligned} a_{ik} &= a_{ik} - \epsilon_k \{ \partial E_j(t) / \partial a_{ik} \} \\ &= a_{ik} - \epsilon_k \{ (\partial E_j(t) / \partial O_j(t)) \{ \partial O_j(t) / \partial a_{ik} \} \} \\ &= a_{ik} + \epsilon_k \{ S_j(t) - O_j(t) \} \{ \partial O_j(t) / \partial a_{ik} \} \end{aligned}$$

[0043]

The equation 2 can be expressed with the equation 4 by the reason that the partial differential value with a_{ik} of the added-up value $O_j(t)$ is given in accordance with the equation 3.

[0044]

[Equation 3]

$$\begin{aligned} \partial O_j(t) / \partial a_{ik} &= \partial \left(\sum_{i=1}^m g_i(t, a_{i1}, a_{i2}, a_{i3}, \dots, a_{iL}) \right) / \partial a_{ik} \\ &= \partial g_i(t, a_{i1}, a_{i2}, a_{i3}, \dots, a_{iL}) / \partial a_{ik} \end{aligned}$$

[0045]

[Equation 4]

$$a_{ik} = a_{ik} + \epsilon_k \{ S_j(t) - O_j(t) \} [\partial g_i(t, a_{i1}, a_{i2}, a_{i3}, \dots, a_{iL}) / \partial a_{ik}]$$

[0046]

From the foregoing description, it is to be understood that the second preferred embodiment of the present invention, which carries out the operation in accordance with Equation 4, can thus improve the accuracy of the estimated vector components. In addition, the corrected value may be set at a negative value when the gradient of the estimated error $dj(t)$ is positive, and may be set at a positive value when the gradient of the estimated error $dj(t)$ is negative. When the vector component of the current element of each vertex is thus obtained, a vector space interpolation processing is carried out based on the current elements of eight vertexes, a magnetic flux density where a minute point occurs is obtained, the magnetic flux density where each of the minute points occurs is integrated, and a magnetic field of each of the small stereoscopic segments is then obtained. Thus, the distributed currents can be displayed with fogs or arrows based on the provided outcome.

[0047]

Furthermore, the process performed by the apparatus shown in FIG. 6 is applicable only to the small stereoscopic segments assigned to the "small stereoscopic segment group to be displayed" obtained by the embodiment shown in FIG. 1 or FIG. 5, thereby largely reducing arithmetical calculations by the reason that the small stereoscopic segments assigned to the "small stereoscopic segment group to be not displayed" correspond to a visceral cavity or the like and are accordingly ignored. Moreover, even if the number of the small stereoscopic segments increases, the number of the vertexes does not increase in proportion to the increased number of the small stereoscopic segments by the reason that one vertex of one small stereoscopic segment serves as the vertex of the adjacent small stereoscopic segment. In the case that the number of the small stereoscopic segments is large enough, the number of the vertexes and the number of the small stereoscopic segments are approximately equal to each other. This also leads to the fact that the present embodiment can reduce the operation load.

[0048]

According to the present invention, the vector components can be sufficiently estimated with a comparatively small number of the measuring points although it has been generally believed that the number of measuring points is required to be greater than the number of unknown values in order to obtain unknown magnetic field-measured values. This also leads to the fact that the present embodiment can decrease the number of measuring points, thereby as a whole reducing the operation load.

[0049]

The following description will be directed to the above-mentioned aspect in detail. Conventionally, internal organs has not been defined as aggregations of small stereoscopic segments, and, for example, the number of measuring points is required to be not less than the number of the current elements to be estimated. This results in the fact that number of the measuring points tends to be more than required especially when the number of the current elements is unknown. The number of the current

elements could not but become enormous by the reason that the currents flowing in the internal organs vary in position, direction, and absolute value with the course of time. In the present embodiment, on the other hand, since the position of each of the small stereoscopic segments is fixed in advance; the current element for a small stereoscopic segment, which does not influence the measuring point, converges on a zero vector. The current element, which has converged on the zero vector, is not required to be processed later. This leads to the fact that the present embodiment of the organism magnetic field measuring apparatus can accurately estimate the vector components based on magnetic field-measured values obtained at a relatively small number of measuring points.

[0050]

Referring now to the drawings, in particular to FIG. 7 of a block diagram, there is shown another preferred embodiment of the organism magnetic field measuring apparatus according to the present invention, and in particular to FIG. 8 of a schematic diagram, there is shown a detailed construction of a part corresponding to a hierarchical type perceptron. The present embodiment of the organism magnetic field measuring apparatus is as shown in FIGS. 7 and 8 comprising: a plurality of hierarchical type perceptrons $10p$ ($p=1,2, \dots, m$) each having a plurality of inputs terminals and one output terminal, an adding unit 200 for adding up function values g_{ij} outputted from the respective hierarchical type perceptrons $10p$, a function value error calculator 300 for calculating a difference between the added-up outcome $Oj(t)$ outputted from the adding unit 200 and a measuring value $Sj(t)$ inputted as a teacher pattern, a plurality of partial differential value calculating units $10pr$ ($r=1,2, \dots, n$) each for calculating a partial differential value corresponding to the function value g_{ij} outputted from the hierarchical type perceptron $10p$, a partial differential value error calculator $30pr$ each for calculating a difference between an output from the partial differential value calculating unit $10pr$ of the hierarchical type perceptron $10p$ and a partial differential value (a partial differential value teacher pattern) calculated in advance in accordance with the numerical differentiation method, a partial differential function learning unit $60p$ each for having the applicable hierarchical type perceptron $10p$ learn a partial differential function based on the difference calculated by the function value error calculator 300 and the difference calculated by the partial differential value error calculator $30pr$, a plurality of correcting units $12p$ each for correcting data to be inputted into the input layer of the hierarchical type perceptron $10p$ (hereinafter referred to as "input data of the hierarchical type perceptron $10p$ ") based on the difference between the added-up outcome $Oj(t)$ calculated by the function value error calculator 300 and the measured value $Sj(t)$ as the teacher pattern, and based on the partial differential value calculated by the partial differential value calculating unit $10pr$, a control unit 400 for selecting a correcting unit $12p$ and a partial differential function learning unit $60p$ from among the plurality of the correcting units $12p$ and partial differential function learning units $60p$ and controlling the correcting unit $12p$ and the partial differential function learning unit $60p$ thus selected to have the selected correcting unit $12p$ and the selected partial differential function learning unit

60p operate repeatedly for a predetermined number of times (until the difference becomes small enough), and a data collecting unit 500 for outputting the input data of the respective hierarchical type perceptrons 10p corresponding to unknown vector components as unknown quantity estimated outcomes under the condition that the input data of the hierarchical type perceptrons 10p has been corrected by the correcting units 12p for the predetermined number of times. It is herein assumed that each of the hierarchical type perceptrons 10p has sufficiently learned functions based on the Biot-Savart law with known input patterns and teacher patterns. Furthermore, the operations of the hierarchical type perceptrons 10p may be performed synchronously or asynchronously.

[0051]

Furthermore, each of the partial differential function learning units 60p is adapted to alternately repeat the two ways of learning: namely, the learning of the hierarchical type perceptron 10p based on the difference calculated by the function value error calculator 300 (for example, a learning of back propagation) and the learning of the hierarchical type perceptron 10p based on the difference calculated by the partial differential value error calculator 30pr, thereby making it possible for each of the hierarchical type perceptrons 10p to learn the partial differential function without losing the learning results so much.

[0052]

Each of the correcting units 12p is adapted to correct an unknown quantity based on the difference between the added-up outcome $O_j(t)$ calculated by the function value error calculator 300 and the measured value $S_j(t)$ as the teacher pattern, and based on the partial differential value calculated by the partial differential value calculating unit 10pr. The calculating unit 10pr, correcting unit 12p, and the function value error calculator 300 collectively constitute an unknown quantity estimating section. The operation of the unknown quantity estimating section will be described in detail hereinlater. The unknown quantity estimating section is operated to slightly change the input data of one of the hierarchical type perceptrons 10p corresponding to an unknown vector component after the hierarchical type perceptrons 10p have completed the learning based on the Biot-Savart law in order to obtain an output pattern and a corresponding partial differential value. Also, it is assumed that the unknown quantity estimating apparatus has calculated in advance a partial differential value in the case that the known input corresponding to the unknown vector component has been slightly changed in accordance with the numerical differentiation method or the like, and stored therein the partial differential value as a partial differential value teacher pattern. In the condition thus prepared, the control unit 400 is operated to select a partial differential function learning unit 60p from a plurality of partial differential function learning units 60p and control the selected partial differential function learning unit 60p to have the selected partial differential function learning unit 60p operate repeatedly for a predetermined number of times. In the way, a back propagation learning is carried out, and a load and a threshold value of a neuronal component constituting each of the hierarchical type perceptrons 10p is

determined so that a function based on the Biot-Savart law and an operation equivalent to the partial differential numerical arithmetic of the function can be realized.

[0053]

Furthermore, the load and the threshold value thus determined as a learning outcome for the selected hierarchical type perceptrons 10p can be adopted as a load and a threshold value for each of hierarchical type perceptrons other than the selected hierarchical type perceptrons 10p. This leads to the fact that the hierarchical type perceptrons other than the selected hierarchical type perceptrons 10p are not required to learn their partial differential functions, thereby drastically reducing the learning time. After the learning process is completed, in place of the partial differential function learning unit 60p, the control unit 400 is operated to select a correcting unit 12p from among a plurality of correcting units. The data collecting unit 500 is then operated to output the input data of the respective hierarchical type perceptrons 10p corresponding to unknown vector components as unknown quantity estimated outcomes when the input data of the hierarchical type perceptrons 10p has been corrected by the correcting units 12p for the predetermined number of times. As will be seen from the foregoing description, it is to be understood that the present embodiment of the organism magnetic field measuring apparatus can estimate the vector components as accurately as the embodiment shown in FIG. 6.

[0054]

[Fourth Embodiment]

Referring to the drawings, in particular to FIG. 9 of a block diagram, there is shown a fourth embodiment of the organism magnetic field measuring apparatus according to this present invention. The constitutional elements of the present embodiment of the organism magnetic field measuring apparatus as shown in FIG. 9 are the entirely the same as those of the previous embodiment of the organism magnetic field measuring apparatus according to this present invention as shown in FIGS. 7 and 8 except for the fact that the present embodiment of the organism magnetic field measuring apparatus comprises an input changing unit 15p for slightly changing an input, an output storing unit 16p for storing therein an output in response to the input not changed by input changing unit 15p and an output in response to the input changed by the input changing unit 15p, and a difference calculating unit 17p for calculating the difference between the output in response to the input not changed by input changing unit 15p and the output in response to the input changed by the input changing unit 15p, respectively stored in the output storing unit 16p, in place of the partial differential value calculating units 10pr provided in the respective hierarchical type perceptrons in the previous embodiment shown in FIGS. 7 and 8.

[0055]

Accordingly, the present embodiment of the organism magnetic field measuring apparatus can calculate the difference between the output in response to the regular input and the output in response to the slightly changed input. The difference between the output in response to the regular input and the output in response to the slightly changed input corresponds to a partial differential value. This leads to the

fact that the present embodiment of the organism magnetic field measuring apparatus can achieve the same advantage of the previous embodiment shown in FIGS. 7 and 8 while eliminating the need of learning the partial differential function, thereby largely reducing the leaning time.

[0056]

[Fifth Embodiment]

Referring to the drawings, in particular to FIG. 10 of a block diagram, there is shown a unit of a fifth embodiment of the organism magnetic field measuring apparatus according to this present invention. The organism magnetic field measuring apparatus is shown in FIG. 10 as comprising: a plurality of Biot-Savart arithmetical calculating units 11i each for performing an arithmetical calculation in accordance with the Biot-Savart law, a current element collecting unit 40a for collecting vector components of current elements estimated by the Biot-Savart arithmetical calculating units 11i and for outputting the collected vector components as an analysis outcome, a plurality of correction quantity calculating units 41i each for calculating correction quantities Δx , Δy , and Δz on the basis of the three-dimensional coordinate values provided by the method shown in FIG. 1 and/or by the apparatus shown in FIG. 5, a plurality of vertex extracting units 42i each for extracting coordinate of each of the adjacent vertexes, for which the estimated vector component of the current element is to be distributed, the basis of the code of the calculated correction quantities Δx , Δy , and Δz , a plurality of standardizing unit 43i each for standardizing a correction vector calculated based on the correction quantities Δx , Δy , and Δz , a plurality of redistributing ratio calculating unit 44i each for calculating a redistributing ratio based on the absolute value of each component of the standardized correction vectors, a plurality of redistributing units 45i each for redistributing an estimated value to the vector component of the current element estimated for each of the extracted vertexes on the basis of the estimated vector component of the current element estimated and the calculated redistributing ratio, a plurality of estimated value updating units 46i each for updating the estimated vector component of the current element in response to the redistributed estimated value, and a repeat control unit 47 for controlling the Biot-Savart arithmetical calculating unit 11i, the correction quantity calculating unit 41i, the vertex extracting unit 42i, the standardizing unit 43i, the redistributing ratio calculating unit 44i, the redistributing unit 45i and the estimated value updating unit 46i to have the Biot-Savart arithmetical calculating unit 11i, the correction quantity calculating unit 41i, the vertex extracting unit 42i, the standardizing unit 43i, the redistributing ratio calculating unit 44i, the redistributing unit 45i and the estimated value updating unit 46i repeatedly operate until the correction quantities Δx , Δy , and Δz becomes vanishingly small.

[0057]

The estimated value updating unit 46i is operative to update the estimated vector component of the current not by simply adding the redistribution ratio to the estimated vector component of the current element, but by adding the average of all of the redistribution ratios to the estimated vector component of the current element. The correction quantity calculating unit 41i is operative to calculate the correction quantities Δx , Δy , Δz by computing the partial differential value of the function value calculated by for example Biot-Savart arithmetical calculation units.

[0058]

The operation of the organism magnetic field measuring apparatus thus constructed will be described hereinlater. Each of the Biot-Savart arithmetical calculation units 11i is operated to carry out the computation in accordance with the following equation:

$$g_{ji} = (i/0.4 \delta) \{ (Y_{ji} \times p_{xi} - X_{ji} \times p_{yi}) / R_{ji}^3 \}$$

where $i/0$ is intended to mean a magnetic permeability, i ($i=1, 2, \dots, N$) is intended to mean the current element contained in each vertex of the respective small stereoscopic segments, j ($j=1, 2, \dots, m$) is intended to mean measuring points. When it is assumed that the measuring condition of each of the measuring points is represented by $P_j = (x_j, y_j, z_j)$ and the unknown physical quantity of each of the current elements is represented by $U_i = (x_i, y_i, z_i, p_{xi}, p_{yi})$, the following equation is derived.

$$X_{ji} = x_j - x_i, Y_{ji} = y_j - y_i, Z_{ji} = z_j - z_i, \text{ and } R_{ji} = (X_{ji}^2 + Y_{ji}^2 + Z_{ji}^2)^{1/2}.$$

[0059]

Thus, the partial differential values of the above-mentioned equations partially differentiated with the respective unknown quantities can be obtained by supplying the correction quantity calculating units 41 with the outcome respectively outputted from the Biot-Savart arithmetical calculating units 11i. The partial differential values can be computed in accordance with the following Equations 5 through 9.

[0060]

[Equation 5]

$$\frac{\partial g_{1j}}{\partial x_i} = \frac{\mu_0}{4\pi} \left\{ \frac{3Y_{ji}(Y_{ji}P_{xi} - X_{ji}P_{yi}) + R_{ji}^{-2}p_{yi}}{R_{ji}^5} \right\}$$

[0061]

[Equation 6]

$$\frac{\partial g_{1j}}{\partial y_i} = \frac{\mu_0}{4\pi} \left\{ \frac{3Y_{ji}(Y_{ji}P_{yi} - X_{ji}P_{xi}) - R_{ji}^{-2}p_{xi}}{R_{ji}^5} \right\}$$

[0062]

[Equation 7]

$$\frac{\partial g_{1j}}{\partial z_i} = \frac{\mu_0}{4\pi} \left\{ \frac{3Z_{ji}(Y_{ji}P_{xi} - X_{ji}P_{yi})}{R_{ji}^5} \right\}$$

[0063]

[Equation 8]

$$\frac{\partial g_{i,j}}{\partial P_{x,i}} = \frac{\mu_0}{4\pi} \frac{Y_{j,i}}{R_{j,i}^3}$$

[0064]

[Equation 9]

$$\frac{\partial g_{i,j}}{\partial P_{y,i}} = \frac{\mu_0}{4\pi} \frac{X_{j,i}}{R_{j,i}^3}$$

[0065]

The correction quantities Δx , Δy , Δz can be obtained based on the partial differentiation computation carried out in accordance with the Equations 5 through 7 and $S_j - O_j$. With the correction quantities Δx , Δy , Δz thus obtained, the adjacent vertexes, for which the estimated vector components of the current elements are to be distributed, can be extracted by the vertex extracting unit 42i based on the codes of the correction quantities Δx , Δy , Δz . As best shown in FIG. 11, concretely, vertexes respectively shown by double circles are extracted as adjacent vertexes, for which the estimated vector components of the current elements are to be distributed, by the fact that the correction vectors respectively shown by dotted lines are obtained. The correction vectors are then standardized by the standardizing unit 43i, the redistributing ratio is calculated by the redistributing ratio calculating unit 44i based on the absolute value of each component of the standardized correction vectors, and an estimate is redistributed by the redistributing unit 45i to the vector component of the current element estimated for each of the extracted vertexes extracted by the extracting unit 42i. In this case, each of the vector components of the current elements may be drastically redistributed on the basis of a plurality of correction vectors. Simply adding the vector components of the current elements may result in the fact that the value before the redistribution is by far different from the value after the redistribution, thereby undermining the reliability of the stability of the estimation. In order to solve this problem, the estimated value updating unit 46i is operative to update the estimated vector component of the current by adding to the estimated vector component of the current element the average of all of the redistribution ratios calculated based on a plurality of standardized correction vectors.

[0066]

The repeat control unit 47 is operated to control the Biot-Savart arithmetical calculating unit 11i, the correction quantity calculating unit 41i, the vertex extracting unit 42i, the standardizing unit 43i, the redistributing ratio calculating unit 44i, the redistributing unit 45i and the estimated value updating unit 46i to have the Biot-Savart arithmetical calculating unit 11i, the correction quantity calculating unit 41i, the vertex extracting unit 42i, the standardizing unit 43i, the redistributing ratio calculating unit 44i, the redistributing unit 45i and the estimated value updating unit 46i repeatedly operate until the correction quantities Δx , Δy , and Δz becomes vanishingly small for

all of the vertexes, thereby highly improve the accuracy of the estimates of the current elements. While the estimation process is performed by the repeat control unit 47, Equation 5, Equation 6, and Equation 7 are not directly influenced by the correction quantities Δx , Δy , Δz by the reason that the three-dimensional coordinate values of each vertex of the respective small stereoscopic segments are to be fixed. The aforementioned equations are, on the other hand, indirectly influenced by the correction quantities Δx , Δy , Δz by the fact that the vector components of the current elements are changed through the redistribution process. This means that through out the processes carried out in accordance with Equation 5, Equation 6, Equation 7, Equation 8, and Equation 9, X_{ji} , Y_{ji} , Z_{ji} , and R_{ji} , remain unchanged while, on the other hand, only p_{xi} and p_{yi} are changed, thereby ensuring that the highly estimated p_{xi} and p_{yi} are obtained. The conventional organism magnetic field measuring apparatus tends to remain currents canceling each other at positions at which in fact no current flows even if the currents canceling each other are placed in the vicinity of each other as shown, for example, in FIG. 12(A). The present embodiment of the organism magnetic field measuring apparatus, on the other hand, carries out the redistribution process, thereby making it possible for the currents canceling each other to be displayed at positions at which actually the currents flow as shown in FIG. 12(B). In FIGS. 12(A) and 12(B), a black dot is intended to mean a vertex to be processed and a circle is intended to mean a vertex placed in the vicinity of the vertex.

[0067]

Examples of the magnetic field source estimating outcomes obtained approximately at the time the Q wave occurs based on magnetic field distribution maps are shown in FIGS. 14 to 18. The magnetic field distribution maps have been prepared by synchronously adding a plurality of magnetocardiograms measured at 3 cm intervals with 6 x 6 points to an electrocardiography using a one-channel magneto meter. As will be seen from FIGS. 14 to 18, it is to be understood that the magnetic field source estimating outcomes precisely represent a cardiac volume current, which is medically confirmed, with a high degree of accuracy. FIG. 13 show information on vertexes with depth of 6 cm obtained based on MRI pictorial images. FIGS. 14 to 18 show estimating outcomes respectively obtained at the time 35 msec, 33 msec, 30 msec, 25 msec, and 20 msec prior to the occurrence of R wave. The large black dots collectively represent a cardiac wall, and line segments respectively originating from the black dots represent current elements.

[0068]

In the present embodiment of the organism magnetic field measuring apparatus according to the present invention, the hierarchical type perceptrons may be adopted in place of the Biot-Savart arithmetical calculating units.

[0069]

[Seventh Embodiment]

Referring to the drawings, in particular to FIG. 19 of a flowchart, there is

shown a seventh preferred embodiment of the organism magnetic field measured outcome display method according to this present invention. As shown in FIG. 19, the organism magnetic field measured outcome display method comprises the steps of: waiting for receiving the position and the magnitude (the absolute value of an excitation current) of the current element in a plane corresponding to the tomogram image at a predetermined point of time (step SP 1), assigning a circle having a diameter corresponding to the magnitude of each of a plurality of the current elements to each of the current elements (step SP 2), displaying the organism tomogram image (step SP 3), displaying the circle assigned to each of the current elements along with the organism tomogram image for each of vivo points (step SP 4), judging whether or not the end of the excitation current display is instructed (step SP 5), and waiting for receiving the position and the magnitude of the current element in a plane corresponding to the tomogram image at another point of time when it is judged in the step SP5 that the end of the excitation current display is not instructed (step SP 6). Then, the step SP6 goes back to the step SP2. When it is, on the other hand, judged in the step SP5 that the end of the excitation current display is not instructed, the process goes to END. In the step SP2, the diameter of the circle assigned to each of the current elements may precisely correspond to the magnitude of each of the current elements. Alternatively, the magnitude of each of the current elements may be divided into a plurality of magnitude grades, and the diameter of the circle assigned to each of the current elements may correspond to the magnitude grade of each of the current elements.

[0070]

[Eighth Embodiment]

Referring to the drawings, in particular to FIG. 20 of a flowchart, there is shown an eighth preferred embodiment of the organism magnetic field measured outcome display method according to this present invention. The organism magnetic field measured outcome display method comprises the steps of: waiting until a point at which an internal organ is placed is detected on a plane corresponding to the tomogram image (step SP 1), assigning a circle having a predetermined diameter to the detected point at which the internal organ is placed (step SP 2), waiting until the position and the magnitude of each of the current elements is obtained at a predetermined point of time on the above-mentioned plane (step SP 3), replacing the circle assigned to the point in the step SP2 with a high-lightened circle having a diameter corresponding to the magnitude of each of the current elements (step SP 4), displaying the organism tomogram image (step SP 5), displaying the circle assigned to the detected point along with the organism tomogram image at the detected point (step SP 6), judging whether or not the end of the excitation current display is instructed (step SP 7), and waiting for the position and the magnitude of the current element in a plane corresponding to the tomogram image at another point of time when it is judged in the step SP7 that the end of the excitation current display is not instructed (step SP 8). Then, the step SP8 goes back to the step SP4. When it is, on the other hand, judged in the step SP7 that the end of the excitation current display is not instructed, the process goes to END.

[0071]

Examples of the excitation currents displayed by the present embodiment of the organism magnetic field measured outcome display method are shown in FIG. 21. As will be seen from FIG. 21, the excitation currents are remarkably visible. The circles are displaced at the point at which the internal organ is placed. In addition, a clearance between the circles is enlarged, thereby making it possible for an operator to recognize the tomogram image as a background. In particular, the present embodiment of the organism magnetic field measured outcome display method can display the excitation currents on the time series, thereby making it possible for an operator to easily recognize, for example, the condition of the maximal excitation current in the process of changing.

[0072]

[Ninth Embodiment]

Referring to the drawings, in particular to FIG. 22 of a flowchart, there is shown a ninth preferred embodiment of the organism magnetic field measured outcome display method according to this present invention. The organism magnetic field measured outcome display method comprises the steps of: waiting for receiving the position and the magnitude of the current element at a predetermined point of time (step SP 1), assigning a sphere having a diameter corresponding to the magnitude of each of a plurality of the current elements to each of the current elements (step SP 2), three-dimensionally displaying a semi-transparent organism structure reference image (step SP 3), displaying the sphere assigned to each of the current elements along with the semi-transparent organism structure reference image for each of corresponding points (step SP 4), judging whether or not the end of the excitation current display is instructed (step SP 5), and waiting for receiving the position and the magnitude of the current element at another point of time when it is judged in the step SP5 that the end of the excitation current display is not instructed (step SP 6). Then, the step SP6 goes back to the step SP2. When it is, on the other hand, judged in the step SP5 that the end of the excitation current display is not instructed, the process goes to END.

[0073]

As will be seen from the foregoing description, it is to be understood that the present embodiment of the organism magnetic field measured outcome display method according to the present invention can display the sphere having a diameter corresponding to the magnitude of each of a plurality of the current elements along with the semi-transparent organism structure reference image for each of corresponding points on the time series, thereby making it possible for an operator to easily recognize the three-dimensional propagation direction of the excitation current.

[0074]

[Tenth Embodiment]

Referring to the drawings, in particular to FIG. 23 of a block diagram, there is shown a tenth preferred embodiment of the organism magnetic field measured outcome displaying apparatus according to this present invention. The organism magnetic field measured outcome displaying apparatus is shown in FIG. 23 as comprising: an

analyzed outcome storing unit 600 for storing therein current elements analyzed outcomes, a circle assigning unit 700 for assigning a circle having a diameter corresponding to the magnitude of each of current elements to each of the current elements, a tomogram image displaying unit 800 for displaying an organism tomogram image, a circle displaying unit 900 for displaying the assigned circle having a diameter corresponding to the magnitude of each of a plurality of the current elements along with the organism tomogram image.

[0075]

As will be seen from the foregoing description, it is to be understood that the present embodiment of the organism magnetic field measured outcome displaying apparatus thus constructed can display the circle having a diameter corresponding to the magnitude of each of a plurality of the current elements along with the organism tomogram image, thereby remarkably increase the visibility of the excitation currents. Furthermore, the present embodiment of the present embodiment of the organism magnetic field measured outcome displaying apparatus can display the circle along with the organism tomogram image on the time series, thereby making it possible for an operator to easily recognize the three-dimensional propagation direction of the excitation current. In the previous seventh to tenth embodiment according to the present invention, the circle may be replaced with a square, a cube, or the like as long as degrease in visibility is admitted to some extend. It will be understood by those skilled in the art that the foregoing description is in terms of preferred embodiment of the present invention wherein various changes and modification may be made without departing from the spirit and scope of the invention, as set forth in the appended claims.

[0076]

[Effects of the Invention]

As will be seen from the foregoing description, it is to be understood, the tomogram image processing method as set forth in claim 1 comprising the steps of: a) carrying out an interpolation operation on a plurality of tomogram images of a test boy sliced in an area at predetermined intervals to obtain stereoscopic image data elements; b) dividing said area into small stereoscopic segments; c) counting the number of said stereoscopic image data elements for each of said small stereoscopic segments; and d) binarizing said small stereoscopic segments on the basis of the number of said stereoscopic image data elements, has an effect of obtaining the stereoscopic image data elements corresponding to all of the small stereoscopic segments by carrying out the interpolation operation on a plurality of tomogram images of the test body even through some tomogram images sliced at the intervals should fail to be provided. Further, the tomogram image processing method thus constructed can obtain a simplified stereoscopic image by the reason that the small stereoscopic segments are binarized on the basis of the number of the stereoscopic image data elements. This leads to the fact that the stereoscopic image obtained and displayed by the tomogram image processing method as set forth in claim 1 makes it possible for an operator to easily distinguish an area and/or a stereoscopic segment where an internal organ or the

like is placed.

[0077]

A tomogram image processing apparatus as set forth in claim 2, comprising: interpolation carrying out means (3) for carrying out an interpolation operation on a plurality of tomogram images of a test boy sliced in an area at predetermined intervals to obtain stereoscopic image data elements; area dividing means (7) for dividing said area into small stereoscopic segments; stereoscopic image counting means (8) for counting the number of said stereoscopic image data elements for each of said small stereoscopic segments; and binarizing means (9, 10) for binarizing said small stereoscopic segments on the basis of the number of said stereoscopic image data elements has an effect of obtaining the stereoscopic image data elements corresponding to all of the small stereoscopic segments by carrying out the interpolation operation on a plurality of tomogram images of the test body even through some tomogram images sliced at the intervals should fail to be provided. Further, the tomogram image processing apparatus thus constructed can obtain a simplified stereoscopic image by the reason that the small stereoscopic segments are binarized on the basis of the number of the stereoscopic image data elements. This leads to the fact that the stereoscopic image obtained and displayed by the tomogram image processing apparatus as set forth in claim 2 makes it possible for an operator to easily distinguish an area and/or a stereoscopic segment where an internal organ or the like is placed.

[0078]

The organism magnetic field measuring method as set forth in claim 3, has an effect of obtaining the data on the magnetic field source for each of a plurality of vertexes of said small stereoscopic segments by the reason that data on said magnetic field sources included in the results of the Biot-Savart law calculations is corrected until the difference between said calculated magnetic field value and a measured magnetic field value becomes vanishingly small. Furthermore, the number of unknown factors to be estimated can be largely reduced in comparison with the conventional method by the reason that the position of each of the vertexes of the small stereoscopic segments is known. The organism magnetic field measuring method thus constructed decreases the number of measuring points, thereby as a whole reducing the operation load. The organism magnetic field measuring method as set forth in claim 4 has an effect of obtaining accurate information on the magnetic field source by the reason that even magnetic field source vectors assigned in positions adjoining to each other, equal to each other in magnitude but opposing to each other in direction can be calibrated. Furthermore, the organism magnetic field measuring method thus constructed decreases the number of measuring points by the reason that one vertex of one small stereoscopic segment serves as the vertex of the adjacent small stereoscopic segment, thereby as a whole reducing the operation load.

[0079]

The organism magnetic field measuring apparatus as set forth in claim 5, has an effect of obtaining the data on the magnetic field source for each of a plurality of vertexes of said small stereoscopic segments by the reason that data on said magnetic

field sources included in the results of the Biot-Savart law calculations is corrected until the difference between said calculated magnetic field value and a measured magnetic field value becomes vanishingly small. Furthermore, the number of unknown factors to be estimated can be largely reduced in comparison with the conventional apparatus by the reason that the position of each of the vertexes of the small stereoscopic segments is known. The organism magnetic field measuring apparatus thus constructed degrades the number of measuring points, thereby as a whole reducing the operation load. The organism magnetic field measuring apparatus as set forth in claim 6 has an effect of obtaining accurate information on the magnetic field source by the reason that even magnetic field source vectors assigned in positions adjoining to each other, equal to each other in magnitude but opposing to each other in direction can be calibrated. Furthermore, the organism magnetic field measuring apparatus thus constructed degrades the number of measuring points by the reason that one vertex of one small stereoscopic segment serves as the vertex of the adjacent small stereoscopic segment, thereby as a whole reducing the operation load.

[0080]

The organism magnetic field-measured outcome display method as set forth in claim 7 of displaying an organism magnetic field-measured outcome along with an organism structure reference image, has an effect of making it possible for an operator to recognize, for example, the distributed condition of the maximal organism magnetic field-measured outcome in comparison with the case that the magnetic field measured outcome is displayed with the direction and the length of the arrows. Moreover, the organism magnetic field-measured outcome display method thus constructed can dynamically display the organism magnetic field measured outcome, thereby making it possible for an operator to easily recognize, for example, the time-variant fluctuation of the distributed condition of the maximal organism magnetic field measured outcome. The organism magnetic field-measured outcome display method as set forth in claim 8, in which the reference graphic is in the form of a circular shape, has an effect of considerably enlarging a clearance between the reference graphics, thereby making it possible for an operator to recognize the organism structure reference image as a background.

[0081]

The organism magnetic field-measured outcome display apparatus as set forth in claim 9 for displaying an organism magnetic field-measured outcome along with an organism structure reference image, has an effect of making it possible for an operator to recognize, for example, the distributed condition of the maximal organism magnetic field-measured outcome in comparison with the case that the magnetic field measured outcome is displayed with the direction and the length of the arrows. Moreover, the organism magnetic field-measured outcome display apparatus thus constructed can dynamically display the organism magnetic field measured outcome, thereby making it possible for an operator to easily recognize, for example, the time-variant fluctuation of the distributed condition of the maximal organism magnetic field measured outcome.

[0082]

The organism magnetic field-measured outcome display apparatus as set forth in claim 10, in which the reference graphic is in the form of a circular shape, has an effect of considerably enlarging a clearance between the reference graphics, thereby making it possible for an operator to recognize the organism structure reference image as a background.

[Brief Description of the Drawings]

The objects, features, and advantages of an imaging device correcting apparatus according to the present invention will become apparent as the description proceeds when taken in conjunction with the accompanying drawings.

[0083]

FIG. 1 is a flowchart showing a preferred embodiment of the tomogram image processing method according the present invention.

[0084]

FIG. 2 is a schematic diagram showing an example of a tomogram image.

[0085]

FIG. 3 is a plan view diagrammatically explaining a relationship between small stereoscopic segments belonging to a small stereoscopic segment group to be displayed and a small stereoscopic segment group to be displayed.

[0086]

[FIG. 4]

It is a perspective view corresponding to FIG. 3.

[0087]

FIG. 5 is a block diagram showing a preferred embodiment of the tomogram image processing apparatus according to the present invention.

[0088]

FIG. 6 is a block diagram showing a preferred embodiment of the organism magnetic field measuring apparatus according to the present invention.

[0089]

FIG. 7 is a block diagram showing another preferred embodiment the organism magnetic field measuring apparatus according to the present invention.

[0090]

FIG. 8 is a schematic diagram showing the detailed construction of the part corresponding to one hierarchical type perceptron.

[0091]

FIG. 9 is a block diagram showing another preferred embodiment the organism magnetic field measuring method according to the present invention.

[0092]

FIG. 10 is a block diagram showing yet another embodiment of the magnetic field source measuring apparatus according to the present invention.

[0093]

FIG. 11 is a schematic diagram explaining a process for extracting an adjacent vertex, for which an estimated vector component of a current element is to be

distributed.

[0094]

FIG. 12 is a schematic diagram explaining a process for estimating a current element carried out during a redistribution operation.

[0095]

FIG. 13 is an illustration representing information on vertexes with depth of 6 cm obtained based on MRI pictorial images.

[0096]

FIG. 14 is an illustration showing an estimating outcome obtained at the time 35 msec prior to the occurrence of R wave.

[0097]

FIG. 15 is an illustration showing an estimating outcome obtained at the time 33 msec prior to the occurrence of R wave.

[0098]

FIG. 16 is an illustration showing an estimating outcome obtained at the time 30 msec prior to the occurrence of R wave.

[0099]

FIG. 17 is an illustration showing an estimating outcome obtained at the time 25 msec prior to the occurrence of R wave.

[0100]

FIG. 18 is an illustration showing an estimating outcome obtained at the time 20 msec prior to the occurrence of R wave.

[0101]

FIG. 19 is a flowchart showing a preferred embodiment of the organism magnetic field-measured outcome display method according to the present invention.

[0102]

FIG. 20 is a flowchart showing another preferred embodiment of the organism magnetic field-measured outcome display method according to the present invention.

[0103]

FIG. 21 is an illustration showing examples of excitation currents displayed by the embodiment shown in FIG. 20.

[0104]

FIG. 22 is a flowchart showing another preferred embodiment of the organism magnetic field-measured outcome display method according to the present invention.

[0105]

FIG. 23 is a block diagram showing an excitation current displaying apparatus as a preferred embodiment of the organism magnetic field-measured outcome displaying unit according to the present invention.

[0106]

[Description of Notations]

3 Tomogram image interpolating unit

7 stereoscopic segment assigning unit

8 pixel number counting unit

9 judging unit
10 display-stereoscopic segment assigning unit
20, 200 adding unit
30, 300 error calculator
41i correction quantity calculating unit
42i vertex extracting unit
43i standardizing unit
44i redistributing ratio calculating unit
45i redistributing unit
46i estimated value updating unit
40, 500 data collecting unit
101,102, ...,10m hierarchical type perceptrons
111,112, ...,11m Biot-Savart arithmetical calculating unit
111a,112a, ...,11ma, 121,122, ...,12m correcting unit
700 circle assigning unit
800 tomogram image displaying unit
900 circle displaying unit

ABSTRACT OF THE DISCLOSURE

PURPOSE:

To obtain a solid model from tomogram images

CONSTITUTION:

The construction of the foregoing methods according to the present invention comprising the steps of: performing interpolation arithmetical calculation on tomogram images taken at respective predetermined intervals of an object such as, for example, internal organs to obtain stereoscopic image data elements, generating small stereoscopic segments in correspondence with the tomogram images and/or interpolation tomogram images to count pixel numbers contained in each of the small stereoscopic segments, assigning the small stereoscopic segments to a display-stereoscopic segment only when the counted value of the pixel numbers is larger in number than a predetermined threshold, and visually displaying only the small stereoscopic segment assigned to the display-stereoscopic segment.

PATENT ABSTRACTS OF JAPAN

(11)Publication number : 06-028455

(43)Date of publication of application : 04.02.1994

(51)Int.Cl.

G06F 15/62

A61B 5/055

// G09G 5/36

(21)Application number : 04-235534

(71)Applicant : DAIKIN IND LTD

(22)Date of filing : 03.09.1992

(72)Inventor : UEDA TOMOAKI

(30)Priority

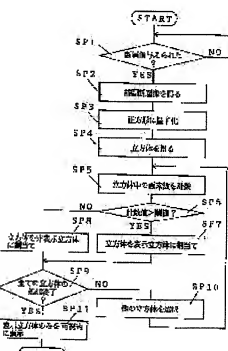
Priority number : 04122295 Priority date : 14.05.1992 Priority country : JP

(54) TOMOGRAPHIC IMAGE PROCESSING METHOD, LIVING BODY MAGNETIC FIELD MEASURING METHOD, LIVING BODY MAGNETIC FIELD MEASURING RESULT DISPLAY METHOD AND DEVICES THEREFOR

(57)Abstract:

PURPOSE: To obtain delicate image data, based on a tomographic image at every prescribed interval by dividing a space which becomes a processing object into prescribed small stereoscopic areas, counting stereoscopic image data contained in each small stereoscopic area, and binarizing the small stereoscopic area based on a counting value.

CONSTITUTION: Based on a tomographic image at a prescribed interval, an interpolating operation is executed and stereoscopic image data is obtained (SP4). A space which becomes a processing object is divided into prescribed small stereoscopic areas, stereoscopic image data contained in each stereoscopic area is counted (SP5), and based on a counting value, the small stereoscopic area is binarized. Even if only the tomographic image at every prescribed interval is obtained, the stereoscopic image data is obtained so as to correspond to all spaces by executing an interpolating operation, and also, by binarizing the small stereoscopic area based on the number of stereoscopic image data contained in the divided small stereoscopic areas, a simplified stereoscopic image can be obtained. Accordingly, in the case where the displayed is executed visibly, the part corresponding to internal organs, etc., and the part corresponding to the space can be recognized simply.



LEGAL STATUS

[Date of request for examination] 31.07.1996

[Date of sending the examiner's decision of rejection] 19.10.1999

[Kind of final disposal of application other than the examiner's decision of rejection or application converted registration]

[Date of final disposal for application]
[Patent number] 3084951
[Date of registration] 07.07.2000
[Number of appeal against examiner's decision of rejection] 11-18535
[Date of requesting appeal against examiner's decision of rejection] 18.11.1999
[Date of extinction of right]

Copyright (C) 1998,2003 Japan Patent Office

(19)日本国特許庁 (JP)

(12) 公開特許公報 (A)

(11)特許出願公開番号

特開平6-28455

(43)公開日 平成6年(1994)2月4日

(51)Int.Cl.⁵
G 0 6 F 15/62
A 6 1 B 5/055
// G 0 9 G 5/36

識別記号 3 9 0 B 9287-5L
9177-5G
8932-4C

F I
A 6 1 B 5/ 05
3 8 0

技術表示箇所

審査請求 未請求 請求項の数10(全 23 頁)

(21)出願番号

特願平4-235534

(22)出願日

平成4年(1992)9月3日

(31)優先権主張番号 特願平4-122295

(32)優先日 平4(1992)5月14日

(33)優先権主張国 日本 (JP)

(71)出願人 000002853

ダイキン工業株式会社

大阪府大阪市北区中崎西2丁目4番12号

梅田センタービル

(72)発明者 上田 智章

滋賀県草津市岡本町字大谷1000番地の2

ダイキン工業株式会社滋賀製作所内

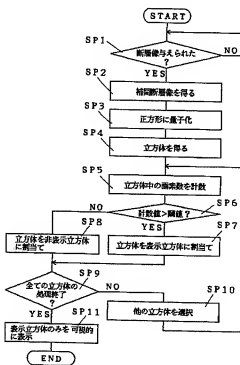
(74)代理人 弁理士 津川 友士

(54)【発明の名称】 断層像処理方法、生体磁場測定方法、生体磁場測定結果表示方法およびこれらの装置

(57)【要約】

【目的】 断層像に基づいてソリッドモデルを得る。

【構成】 所定間隔毎の断層像に基づいて補間演算を行なって補間断層像を得、断層像または補間断層像に対応させて小立方体を生成し、各小立方体に含まれる画素数を計数して、計数値が閾値よりも大きい場合にのみ小立方体を表示立方体に割り当て、表示立方体に割当てられた小立方体のみを可視的に表示する。



【特許請求の範囲】

【請求項1】 所定間隔毎の断層像に基づいて補間演算を行なって立体像データを得、処理対象となる空間を所定の小立体領域に区分して各小立体領域に含まれる立体像データを計数し、計数値に基づいて小立体領域を2値化することを特徴とする断層像処理方法。

【請求項2】 所定間隔毎の断層像に基づいて補間演算を行なって立体像データを得る断層像補間手段(3)と、処理対象となる空間を所定の小立体領域に区分する空間区分手段(7)と、区分された各小立体領域に含まれる立体像データを計数する立体像データ計数手段(8)と、計数値に基づいて小立体領域を2値化する2値化手段(9)、(10)とを含むことを特徴とする断層像処理装置。

【請求項3】 請求項1の断層像処理方法により得られた小立体領域の頂点の位置情報に基づいて異なる磁場源情報に基づく複数のビオ・サバールの法則の演算を行ない、各演算結果を累積加算して得られる磁場演算値と測定した磁場計測値との差を算出し、算出した差に基づいて各演算式に含まれる磁場源情報を補正し、差が十分に小さくなるまで上記一連の処理を反復してから各演算式に含まれる磁場源情報を生体磁場測定結果として出力することを特徴とする生体磁場測定方法。

【請求項4】 算出した差に基づく補正に代えて、各小立体領域の各頂点の各座標成分の修正量を算出し、各座標成分の修正量の符号に基づいて修正対象頂点を得るとともに、各座標成分の修正量に基づいて、得られた修正対象頂点に対して磁場源情報推定値の再配分を行なう処理を採用する請求項3に記載の生体磁場測定方法。

【請求項5】 請求項1の断層像処理方法により得られた小立体領域の頂点の位置情報に基づいて異なる磁場源情報に基づく複数のビオ・サバールの法則の演算を行なう演算手段(11 1)、(11 2)、(11 m)、(1 0 1)、(1 0 2)、(1 0 m)と、各演算手段(1 1 1)、(1 1 2)、(1 1 m)、(0 1 0)、(0 1 2)、(0 1 m)から出力される演算結果を累積加算する累積加算手段(20)、(2 0 0)と、累積加算手段(20)、(2 0 0)から出力される累積加算結果と磁場計測値を入力として誤差を算出する誤差算出手段

(30)、(3 0 0)と、算出誤差に基づいて各演算手段(1 1 1)、(1 1 2)、(1 1 m)、(0 1 0)、(0 1 2)、(0 1 m)における磁場源情報の補正を行なう補正手段(11 1 a)、(1 1 2 a)、(1 1 m a)、(1 2 1)、(1 2 2)、(1 2 m)と、補正手段(1 1 1 a)、(1 1 2 a)、(1 1 m a)、(1 2 1)、(1 2 2)、(1 2 m)による補正が施された結果を収集して生体磁場測定結果として出力する補正結果収集手段(40)、(5 0 0)とを含むことを特徴とする生体磁場測定装置。

【請求項6】 补正手段として、各小立体領域の各頂点

の各座標成分の修正量を算出する修正量算出手段(4 1 1)と、各座標成分の修正量の符号に基づいて修正対象頂点を抽出する修正対象頂点抽出手段(4 2 i)と、各座標成分の修正量に基づいて、得られた修正対象頂点に対して磁場源情報推定値の再配分を行なう再配分手段(4 3 i)、(4 4 i)、(4 5 i)、(4 6 i)とを含むものを用いる請求項5に記載の生体磁場測定装置。

【請求項7】 生体磁場測定結果を生体構造参照像と共に表示する方法であつて、生体内の複数の点のそれぞれに対応する生体磁場測定値の絶対値に基づいて単位图形のサイズを設定し、生体構造参照像を表示するとともに、生体構造参照像の該当位置に設定されたサイズの単位图形を表示することを特徴とする生体磁場測定結果表示方法。

【請求項8】 単位图形が円である請求項7に記載の生体磁場測定結果表示方法。

【請求項9】 生体磁場測定結果を生体構造参照像と共に表示する装置であつて、生体内の複数の点のそれぞれに対応する生体磁場測定値の絶対値に基づいて単位图形のサイズを設定する単位图形サイズ設定手段(7 0 0)と、生体構造参照像を表示する生体像表示手段(8 0 0)と、生体構造参照像の該当位置に設定されたサイズの単位图形を表示する単位图形表示手段(9 0 0)とを含むことを特徴とする生体磁場測定結果表示装置。

【請求項10】 単位图形が円である請求項9に記載の生体磁場測定結果表示装置。

【発明の詳細な説明】

【0 0 0 1】

【産業上の利用分野】 この発明は断層像処理方法、生体磁場測定方法、生体磁場測定結果表示方法およびこれらの装置に関し、さらに詳細にいえば、所定間隔毎の断層像に基づいてきめ細かい像データを得るために新規な断層像処理方法およびその装置、断層像処理方法により得られたきめ細かい像データに基づいて生体磁場源の解析を行なうための新規な生体磁場測定方法およびその装置、ならびに生体磁場源の解析結果を把握し易い状態で表示するための新規な生体磁場測定結果表示方法およびその装置に関する。

【0 0 0 2】

【従来の技術】 従来から生体磁場解析結果を把握し易い状態で表示するために、MR 1画像等の断層像を可視的に表示した状態で磁場源を可視的に重畳して表示する方法が採用されている。また、磁場源を可視的に重畳表示する方法として、磁場源に最も近い断層像と重畳した状態で磁場源を2次元的に表示する方法および複数の断層像を3次元的に表示し、磁場源をも3次元的に表示する方法が提案されている。

【0 0 0 3】 また、生体磁場測定を測定する方法として、磁場源がシングル・ダイボールであると仮定した場合に対処するための測定方法および磁場源が複数電流素

片であると仮定した場合に對処するための測定方法が提案されている。前者の方法は、体表近傍における複数点の磁場測定結果に基づいてシングル・ダイポールの位置および方向性等を算出する方法である。また、後者の方法は、複数の電流素片（通常は30～100程度の電流素片）の存在を仮定しておき、電流素片の数よりも著しく多い測定点における磁場測定結果に基づいて演算を行ない、上記複数の電流素片の位置および方向性を算出する方法である。

【0004】また、生体磁気計測結果に基づく磁場源解析を行なうことにより得られた電流素片を電流ベクトルとして表示するアーローマップ表示、または、等磁線に基づくコンターマップ表示が知られている。そして、医療解析に用いる場合には、MRI画像上に電流ベクトルを示す矢印、または等磁線をオーバーラップさせて表示することにより、臓器中における電流素片または等磁線を可視的に表示することが提案されている。

【0005】

【発明が解決しようとする課題】上記磁場源表示方法のうち、2次元的に表示する方法を採用した場合には、磁場源が何れかの断層像上に位置する可能性が著しく低いとともに、選択された断層像に対する磁場源の相対位置（特に奥行き方向の相対位置）が全く把握できないのであるから、医師等が2次元的な量表示を見ても磁場源の位置を正確に把握することが非常に困難になってしまいという不都合がある。また、断層像では生体内部の臓器の有無を示しているのであるが、臓器の奥行き方向の形状が断層像の形状からはずれてしまう可能性が高いのであるから、実際には断層像において臓器が存在しない位置に磁場源が表示されてしまう可能性が高くなり、この点からも磁場源の位置を正確に把握することが非常に困難になってしまいます。

【0006】また、3次元的に表示する方法を採用した場合には、基準になる画像として複数の断層像が存在するだけであるから、臓器との位置関係が非常に把握しにくいのみならず、断層像以外に目印がないのであるから、磁場源の深さ、奥行きが非常に把握しにくいという不都合がある。上記生体磁場測定を測定する方法のうち、磁場源がシングル・ダイポールであると仮定した場合に對処するための測定方法を採用した場合には、測定結果としてシングル・ダイポールが得られるだけであるから、臓器の運動時に流れる体積電流に代表される分布性磁場源の測定には対処できないという不都合があるのであると深すぎる解に収束してしまい勝ちであるといふ不都合もある。

【0007】また、磁場源が複数電流素片であると仮定した場合に對処するための方法を採用した場合には、分布性磁場源の測定が可能になるのである。しかし、一般的に、30～100程度の電流素片を想定することが必要になるのであるから、全ての電流素片の測定を行なお

うとすれば、200～1000チャネル程度のアレイセンサを設けて多数の磁場計測値を得、得られた多数の磁場計測値に基づいて各電流素片の推定処理のための演算を行なう必要がある。そして、上述の場合に対する推定処理のための演算負荷はテラ・フロップスが要求されるのであるから、システム全体として著しく大規模になるとともに、高価になってしまいという不都合がある。また、推定処理においてローカルミニマに収束してしまう確率が高く、正確な電流素片の推定を達成できる確率が著しく減少してしまうという不都合もある。

【0008】また、上記アーローマップ表示、等磁線表示の何れも特定のタイミングにおける生体磁場測定値、即ち分布を可視的に表示するものであり、動的な生体磁場測定値の表示には不適切である。さらに詳細に説明すると、アーローマップ表示により動的に電流素片を表示することは可能であるが、一般的に臓器における電流素片の数は、体積電流を表示するのに十分な数に設定しなければならない。即ち、著しく多数の電流素片がベクトル表示されなければならない。そして、これら全ての電流素片の向き、大きさが時々刻々と変化するのであるから、MRI画像とオーバーラップ表示された矢印を見ても、例えば、臓器の興奮電流の伝播状態を簡単に把握できないという不都合がある。

【0009】コンターマップ表示を動的な生体磁場測定値の表示に適用しても、等磁線はもともと個々の電流素片の表示には不向きであるから、到底臓器の興奮電流の伝播状態の把握のために採用することはできない。

【0010】

【発明の目的】この発明は上記の問題点に鑑みてなされたものであり、所定間隔毎の断層像に基づいてきめ細かい像データを得ることができ新規な断層像処理方法およびその装置を提供することを第1の目的とし、断層像処理方法により得られたきめ細かい像データに基づいて簡単にかつ正確に生体磁場源の解析を行なうことができ生体磁場測定方法およびその装置を提供することを第2の目的とし、動的な生体物理量測定値を把握し易い状態で表示できる生体物理量計測結果表示方法およびその装置を提供することを第3の目的としている。

【0011】

【課題を解決するための手段】上記第1の目的を達成するための、請求項1の断層像処理方法は、所定間隔毎の断層像に基づいて補間演算を行なって立体像データを得、処理対象となる空間を所定の小立体領域に区分して各小立体領域に含まれる立体像データを計数し、計数値に基づいて小立体領域を2値化する方法である。

【0012】請求項2の断層像処理装置は、所定間隔毎の断層像に基づいて補間演算を行なって立体像データを得る断層像補間手段と、処理対象となる空間を所定の小立体領域に区分する空間区分手段と、区分された各小立体領域に含まれる立体像データを計数する立体像データ

計数手段と、計数値に基づいて小立体領域を2値化する2値化手段とを含んでいる。

【0013】上記第2の目的を達成するための、請求項3の生体磁場測定方法は、請求項1の断層像処理方法により得られた小立体領域の頂点の位置情報に基づいて異なる磁場源情報に基づく複数のビオ・サバルの法則の演算を行ない、各演算結果を累積加算して得られる磁場演算値と測定した磁場計測値との差を算出し、算出した差に基づいて各演算式に含まれる磁場源情報を補正し、差が十分に小さくなるまで上記一連の処理を反復してから各演算式に含まれる磁場源情報を生体磁場測定結果として出力する方法である。

【0014】請求項4の生体磁場測定方法は、算出した差に基づく補正に代えて、各小立体領域の各頂点の各座標成分の修正量を算出し、各座標成分の修正量の符号に基づいて修正対象頂点を得るとともに、各座標成分の修正量に基づいて、得られた修正対象頂点に対して磁場源情報推定値の再配分を行なう処理を採用する方法である。

【0015】請求項5の生体磁場測定装置は、請求項1の断層像処理方法により得られた小立体領域の頂点の位置情報に基づいて異なる磁場源情報に基づく複数のビオ・サバルの法則の演算を行なう演算手段と、各演算手段から出力される演算結果を累積加算する累積加算手段と、累積加算手段から出力される累積加算結果と磁場計測値とを入力として誤差を算出する誤差算出手段と、算出誤差に基づいて各演算手段における磁場源情報の補正を行なう補正手段と、補正手段による補正が施された結果を収集して生体磁場測定結果として出力する補正結果収集手段とを含んでいる。

【0016】請求項6の生体磁場測定装置は、補正手段として、各小立体領域の各頂点の各座標成分の修正量を算出す修正量算出手段と、各座標成分の修正量の符号に基づいて修正対象頂点を抽出する修正対象頂点抽出手段と、各座標成分の修正量に基づいて、得られた修正対象頂点に対して磁場源情報推定値の再配分を行なう再配分手段とを含むものを用いている。

【0017】上記第3の目的を達成するための、請求項7の生体磁場測定結果表示方法は、生体内の複数の点のそれぞれに対応する生体物理量計測値の絶対値に基づいて単位图形のサイズを設定し、生体構造参照像を表示するとともに、生体構造参照像の該当位置に設定されたサイズの単位图形を表示する方法である。請求項8の生体磁場測定結果表示方法は、円からなる単位图形を表示する方法である。

【0018】請求項9の生体磁場測定結果表示装置は、生体内の複数の点のそれぞれに対応する生体物理量計測値の絶対値に基づいて単位图形のサイズを設定する単位图形サイズ設定手段と、生体構造参照像を表示する生体像表示手段と、生体構造参照像の該当位置に設定された

サイズの単位图形を表示する単位图形表示手段とを含んでいる。請求項10の生体磁場測定結果表示装置は、円からなる単位图形を表示するものである。

【0019】

【作用】請求項1の断層像処理方法であれば、所定間隔毎の断層像に基づいて補間演算を行なって立体像データを得、処理対象となる空間を所定の小立体領域に区分して各小立体領域に含まれる立体像データを計数し、計数値に基づいて小立体領域を2値化するのであるから、所定間隔毎の断層像しか得られていない場合でも、補間演算を行なうことにより全空間に対応して立体像データを得、しかも区分された小立体領域に含まれる立体像データの数に基づいて小立体領域を2値化することにより単純化された立体像を得ることができる。したがって、可視的に表示した場合に、臓器等に相当する箇所、空間に相当する箇所を簡単に認識できる。

【0020】尚、上記補間演算としては、直線補間演算、スプライン補間演算等から適宜選択された補間演算を採用すればよい。また、小立体領域を2値化する場合における立体像データの数についても断層像の種類、対象臓器等に適合させるべく適宜閾値を設定すればよい。さらに、小立体領域としては、空間を密に充填し得る立体領域であればよいが、後処理の簡素化等を考慮すれば、立方体領域であることが最も好ましい。

【0021】請求項2の断層像処理装置であれば、所定間隔毎の断層像に基づいて断層像補間手段により補間演算を行なって立体像データを得る。また、空間区分手段により、処理対象となる空間を所定の小立体領域に区分しておく。そして、立体像データ計数手段により、区分された各小立体領域に含まれる立体像データを計数し、2値化手段により、計数値に基づいて小立体領域を2値化する。可視的に表示した場合に、臓器等に相当する箇所、空間に相当する箇所を簡単に認識できる。請求項3の生体磁場測定方法であれば、請求項1の断層像処理方法により得られた小立体領域の頂点の位置情報に基づいて異なる磁場源情報に基づく複数のビオ・サバルの法則の演算を行ない、各演算結果を累積加算して得られる磁場演算値と測定した磁場計測値との差を算出し、算出した差に基づいて各演算式に含まれる磁場源情報を補正し、差が十分に小さくなるまで上記一連の処理を反復してから各演算式に含まれる磁場源情報を生体磁場測定結果として出力するのであるから、複数のビオ・サバルの法則の演算結果の累積加算値が磁場計測値と高精度に近似されるまで補正を行なうことにより、各小立体領域の頂点における磁場源情報を得ることができる。また、小立体領域の頂点の位置情報は既知であるから、推定すべき未知数の数を大幅に低減できる。

【0022】請求項4の生体磁場測定方法であれば、各小立体領域の各頂点の各座標成分の修正量を算出し、各座標成分の修正量の符号に基づいて修正対象頂点を得る

とともに、各座標成分の修正量に基づいて、得られた修正対象頂点に対する磁場源情報推定値の再配分を行なうことにより、算出した差に基づく補正を行なうのであるから、互に近接する状態で割り当てられた、大きさが互に等しくかつ向きが互に逆の磁場源ベクトルが存在していても、これらを確実に補正でき、一層高精度に推定された磁場源情報を得ることができる。また、隣接する頂点間で再配分を行なうことにより推定を行なうのであるから、推定対象となる磁場源情報の数に見合って從来必要とされていた測定点数よりも少ない測定点に基づいて高精度の磁場源推定を達成できる。

【0023】請求項5の生体磁場測定装置であれば、請求項1の断層像処理方法により得られた小立体領域の頂点の位置情報に基づいて、演算手段により異なる磁場源情報に基づく複数のビオ・サバルの法則の演算を行なって、累積加算手段により、各演算手段から出力される演算結果を累積加算する。そして、累積加算手段から出力される累積加算結果と磁場計測値に基づいて誤差算出手段により誤差を算出し、算出誤差に基づいて補正手段により各演算手段における磁場源情報の補正を行なう。補正手段による補正処理を必要回数だけ行なった後に、補正結果集手段により、補正手段による補正が施された結果を収集して生体磁場測定結果として出力することにより、各小立体領域の頂点における磁場源情報を得ることができる。また、小立体領域の頂点の位置情報は既知であるから、推定すべき未知数の数を大幅に低減でき、装置全体として構成を簡素化できる。

【0024】請求項6の磁場源測定装置であれば、補正量算出手段により各小立体領域の各頂点の各座標成分の修正量を算出し、各座標成分の修正量の符号に基づいて修正対象頂点抽出手段により修正対象頂点を抽出し、再配分手段により、各座標成分の修正量に基づいて、得られた修正対象頂点に対して磁場源情報推定値の再配分を行なうことにより、算出した差に基づく補正を行なうのであるから、互に近接する状態で割り当てられた、大きさが互に等しくかつ向きが互に逆の磁場源ベクトルが存在していても、これらを確実に補正でき、一層高精度に推定された磁場源情報を得ることができる。また、隣接する頂点間で再配分を行なうことにより推定を行なうのであるから、推定対象となる磁場源情報の数に見合って從来必要とされていた測定点数よりも少ない測定点に基づいて高精度の磁場源推定を達成できる。

【0025】生体磁場測定方法についてさらに詳細に説明すると、本件発明が生体磁場の測定に関する観察研究を重ねた結果、次のことを見出した。各小立体領域の各頂点は断層像処理方法により得られているのであるから、座標値は既知である。したがって、各頂点における磁場源情報を得るために必要な情報は電流素片のベクトル成分のみである。

【0026】また、1つの小立体領域の1つの頂点は、

隣合う他の小立体領域の頂点を兼ねているのであるから、小立体領域の数が増加しても、頂点数が小立体領域の増加に比例して増加することなく、小立体領域の数が十分に大きければ、頂点数と小立体領域の数はほぼ等しくなる。さらに、1つの頂点の電流素片は隣接する他の電流素片と相關があるので、1つの頂点の電流素片当たりの情報量は一般的な未知数量の推定を行なう場合と比較して著しく少なくて済む。

【0027】さらにまた、磁場源でない頂点における電流素片は0ベクトルに収束するので、最終的に推定を行なわなければならない電流素片の数は著しく少なくななる。請求項3から請求項6の発明は上記の知見に基づいてなされたものであり、測定開始時点においては未知の電流素片（數も未知）の推定を行なうに当って、未知の電流素片数を考慮することなく、計測システムの能力、容量等に基づいて定まる所定数の磁場計測値を得、所定数の磁場計測値に基づいて磁場源情報の補正処理を反復することにより未知の電流素片の高精度の推定を達成でき、推定結果を生体磁場測定結果として採用できる。

【0028】請求項7の生体磁場測定結果表示方法であれば、生体磁場測定結果を生体構造参照像と共に表示するに当って、生体内の複数の点のそれぞれに対応する生体磁場測定値の絶対値に基づいて単位図形のサイズを設定し、生体構造参照像を表示するとともに、生体構造参照像の該当位置に設定されたサイズの単位図形を表示するのであるから、矢印の方向と長さで磁場測定結果を表示する場合と比較して、例えば、最大の生体磁場測定結果の分布状態を簡単に認識できる。但し、生体磁場の方向成分に関しては把握できないことになるが、生体磁場測定結果を動的に表示すれば、例えば、最大の生体磁場測定結果の分布状態の時間的変動を簡単に認識できるのであるから、特に不都合はない。生体磁場測定結果の表示が最も意味を持つ医療解析においては、一般に最大の生体磁場測定結果の分布および時間的変動を簡単に把握できることが要望されるのであるから、この生体磁場測定結果表示方法はこの要望に最適の方法である。

【0029】請求項8の生体磁場測定結果表示方法であれば、請求項7の作用に加え、単位図形が円であるから、単位図形同士の隙間をかなり大きくでき、背景となる生体構造参照像の把握が容易になる。請求項9の生体磁場測定結果表示装置であれば、生体磁場測定結果を生体構造参照像と共に表示するに当って、生体内の複数の点のそれぞれに対応する生体磁場測定値の絶対値に基づいて単位図形サイズ設定手段により単位図形のサイズを設定し、生体像表示手段により生体構造参照像を表示するとともに、単位図形表示手段により生体構造参照像の該当位置に設定されたサイズの単位図形を表示するのであるから、矢印の方向と長さで磁場測定結果を表示する場合と比較して、例えば、最大の生体磁場測定結果の分布状態を簡単に認識できる。但し、生体磁場の方向成分

に関しては把握できることになるが、生体磁場測定結果を動的に表示すれば、例えば、最大の生体磁場測定結果の分布状態の時間的変動を簡単に認識できるのであるから、特に不都合はない。生体磁場測定結果の表示が最も意味を持つ医療解析においては、一般に最大の生体磁場測定結果の分布および時間的変動を簡単に把握できることが要望されるのであるから、この生体磁場測定結果表示装置はこの要望に最適の装置である。

【0030】請求項10の生体磁場測定結果表示装置であれば、請求項9の作用に加え、単位图形が円であるから、単位图形同士の隙間をかなり大きくでき、背景となる生体構造参照像の把握が容易になる。

【0031】

【実施例】以下、実施例を示す添付図面によって詳細に説明する。図1はこの発明の断層像処理方法の一実施例を説明するフローチャートであり、ステップSP1において断層像が与えられるまで待ち、ステップSP2において、与えられた断層像に基づく補間処理を行なって補間断層像を得、ステップSP3において、与えられた断層像および補間断層像を予め設定されたサイズの正方形に量子化し、ステップSP4において、量子化された正方形の中心を中心とし、かつ1辺が正方形の1辺と等しい立方体を得、ステップSP5において、何れかの立方体について、与えられた断層像を構成する画素および補間断層像を構成する画素の数を計算し、ステップSP6において計数値が予め設定されている閾値（例えば、全平均値の平均値）よりも大きいか否かを判定する。そして、計数値が閾値よりも大きいと判定された立方体についてはステップSP7において表示されるべき立方体（以下、表示立方体と称する）に割り当てる、逆にステップSP6において計数値が閾値よりも大きないと判定された立方体についてはステップSP8において表示されない立方体（以下、非表示立方体と称する）に割り当てる。ステップSP7またはステップSP8の処理が行なわれた後は、ステップSP9において全ての立方体について処理が完了したか否かを判定し、処理が行なわれていない立方体が存在すると判定された場合には、ステップSP10において他の立方体を選択し、再びステップSP5の処理を行なう。また、ステップSP9において全ての立方体について処理が完了したと判定された場合には、ステップSP11において、表示立方体に割り当てられた立方体のみを可視的に表示して一連の処理を終了する。

【0032】但し、立方体に含まれる画素数に代えて、立方体中の全画素数に対する断層像画素数の割合および対応する閾値を採用してもよいことはもちろんである。図2から図4を参考しながら断層像処理方法をさらに説明する。図2は断層像の一例を示す概略図であり、ぬりつぶし表示された部分が人体の臓器を示している。図2に示す断層像について量子化された正方形の中心が小さ

いドットで示されるように与えられるので、与えられたドットを中心とする立方体が定まることになる。そして、定められた立方体に含まれる画素数が閾値よりも大きい場合には図3に平面視して示すように表示立方体と非表示立方体とに割り当てる。図4は図3に対応する斜視図であり、表示立方体に割り当てられた立方体のみが表示されている。したがって、表示された立方体を見ることにより、臓器の立体形状を簡単に把握できる。

【0033】尚、この一連の処理を全ての断層像および補間断層像について行なうことにより、生体臓器をソリッド・モデルとして可視的に表示できる。但し、磁場源解析結果を重畠表示する場合には、磁場源解析結果を確認しやすくするために、表示立方体に割り当てられた立方体を半透明表示することが好ましい。また、断層像中における各臓器を指定することにより、該当する臓器のみの表示、複数の臓器の色分け表示をも簡単に達成できる。さらに、非表示立方体は臓器の空洞等に対応するのであるから、後述する生体磁場源解析等に当たっては表示立方体のみについて処理を行なえばよくなり、後処理に必要な演算負荷を大幅に低減できる。

【0034】

【実施例2】図5はこの発明の断層像処理装置の一実施例を示すブロック図であり、複数の断層像を保持する断層像保持部1と、断層像保持部1から処理対象となる断層像を選択する第1断層像選択部2と、選択された断層像に基づく補間処理を行なって補間断層像を得る断層像補間部3と、補間断層像を保持する補間断層像保持部4と、断層像選択部2および断層像補間部3を必要回数だけ反復動作させる第1反復制御部5と、第1反復制御部5による反復動作制御が終了したことに対応して、断層像保持部1または補間断層像保持部4から順次断層像を選択する第2断層像選択部6と、選択された断層像に対して立方体を割り当てる立方体制り当部7と、割り当てられた立方体中に存在する画素数を計数する画素数計数部8と、計数された画素数が所定の閾値よりも大きいか否かを判定する判別部9と、画素数が所定の閾値よりも大きいことを示す判別部9の判定結果に応答して該当する立方体を表示立方体に割り当てる表示立方体制当部10と、画素数が所定の閾値よりも大きくなることを示す判別部9の判定結果に応答して該当する立方体を非表示立方体に割り当てる非表示立方体制当部11と、断層像、補間断層像に対応して立方体の割当結果を保持する割当結果保持部12と、第2断層像選択部6、立方体制当部7、画素数計数部8、判別部9、表示立方体制当部10および非表示立方体制当部11を必要回数だけ反復動作させる第2反復制御部13と、第2反復制御部13により反復動作制御が終了したことに対応して表示立方体に割り当てられた立方体のみを可視的に表示する立方体表示部14とを有している。

【0035】したがって、図5の構成の断層像処理装置

を採用することにより、図2から図4に示す断層像の処理および表示立方体に割り当てられた立方体のみに基づく可視的表示を達成できる。

[0036]

【実施例3】図6はこの発明の生体磁場測定装置の一実施例を示すブロック図であり、複数個の、ビオ・サバールの法則の演算を行なうビオ・サバール演算ユニット1 11, 1 12, ..., 1 1mと、ビオ・サバール演算ユニット1 1 1, 1 12, ..., 1 1mから出力される演算結果を累積加算するシグマ・ユニット2 0と、シグマ・ユニット2 0から出力される累積加算結果 $O_j(t)$ と教師パターンとしての磁場計測値 $S_j(t)$ とを入力として両者の差を算出する誤差演算器3 0と、算出された差に基づいて、ビオ・サバール演算ユニット1 1 1, 1 12, ..., 1 1mにおいて推定されている電流素片のベクトル成分を補正する補正部1 1 1 a, 1 1 2 a, ..., 1 1 m aと、ビオ・サバール演算ユニット1 1 1, 1 12, ..., 1 1mにおいて推定されている電流素片のベクトル成分を収集して解析結果として出力する情報収集ユニット4 0とを有している。尚、上記ビオ・サバール演算ユニット1 1 1, 1 12, ..., 1 1mは、時刻t、図1の断層像処理方法もしくは図5の断層像処理装置により得られた、表示立方体に割り当てられた立方体の頂点の位置情報が既知情報として供給されたことに応答して、既知情報に基づいて各ビオ・サバール演算ユニットに設定されている。ビオ・サバールの法則の演算を行なうとともに、誤差演算器3 0から出力される推定誤差 $d_j(t) = S_j(t) - O_j(t)$ が供給されたことに応答して演算式に含まれる暖流素片のベクトル成分を推定誤差が少なくなるように補正する。また、ビオ・サバール演算ユニット1 1 1, 1 12, ..., 1 1mはそれぞれ同期的に動作するよう位相制御してもよく、また、非同期的に動作するように制御してもよい。

【0037】上記の構成の生体磁場測定装置の作用は次のとおりである。解析対象となる磁場 $O_j(t)$ は、時刻tと各小立方体の頂点の3次元座標 $x_i, y_i, z_{\theta E_j(t) / \partial O_j(t)} = [S_j(t) - O_j(t)]$

【0041】そして、各ビオ・サバール演算ユニットにおけるベクトル成分の補正を最急降下法に基づいて行なうこととすれば、推定誤差評価関数が最小になるベク

トル成分の推定は数2に基いて行なうことができる。
 $a_{ik} = a_{ik} - \epsilon_k (\partial E_j(t) / \partial a_{ik})$

$$\begin{aligned}
 &= a_{ik} - \epsilon_k [(\partial E_j(t) / \partial O_j(t)) (\partial O_j(t) / \\
 &\partial a_{ik}) - a_{ik} + \epsilon_k (S_j(t) - O_j(t)) (\partial O_j(t) / \\
 &\partial a_{ik})]
 \end{aligned}$$

【0043】また、累積加算値 $O_j(t)$ の a_{ik} による偏微分値は数3で与えられるので、数2は数4と表現できる。

i (iは正の整数、以下同じ) および電流素片のベクトル成分 $P_x i, P_y i, P_z i$ を持つ関数 g_i (ビオ・サバールの法則に基づいて定まる関数) の線形和である。但し、磁場センサとして平面内のベクトル成分のみを計測可能なものを使用する場合には、座標系をセンサに適合させることにより何れかのベクトル成分をオミットできる。また、各小立方体は図1の断層像処理方法または図5の断層像処理装置により得られているのであるから、3次元座標値は全て既知の値である。

【0038】したがって、時刻tおよび各小立方体の各頂点の3次元座標値をm個のビオ・サバール演算ユニット1 1 1, 1 12, ..., 1 1mに供給してそれぞれ関数 g_1, g_2, \dots, g_m の演算を行なって関数値を算出し、算出された全ての関数値をシグマ・ユニット2 0に供給することにより累積加算値 $O_j(t)$ を得ることができる。但し、当初は各電流素片のベクトル成分が適当に設定されているのであるから、得られる累積加算値 $O_j(t)$ は実際の計測値 $S_j(t)$ とは異なる。したがって、誤差演算器3 0において実際の計測値 $S_j(t)$ と累積加算値 $O_j(t)$ との差を算出し、算出された差を推定誤差 $d_j(t)$ としてビオ・サバール演算ユニット1 1 1, 1 12, ..., 1 1mの補正部1 1 1 a, 1 1 2 a, ..., 1 1 m aにフィードバックし、推定誤差 $d_j(t)$ が小さくなるように各ビオ・サバール演算ユニットのベクトル成分を変化させる。

【0039】上記一連の処理を反復すれば推定誤差 $d_j(t)$ が小さくなり、ついには推定誤差 $d_j(t)$ がほぼ0になるので、この時点においてビオ・サバール演算ユニットのベクトル成分の値を情報収集ユニット4 0により収集して出力することにより各小立方体の各頂点における電流素片のベクトル成分を得ることができる。また、推定誤差評価関数 $E_j(t)$ を次式で定義すれば、 $E_j(t)$ が得られる。

$$E_j(t) = (1/2) \{S_j(t) - O_j(t)\}^2$$

[0040]

【数1】

$$a_{ik} = a_{ik} - \epsilon_k (S_j(t) - O_j(t))$$

但し、 ϵ_k はベクトル成分 a_{ik} の学習ゲイン (補正ゲイン) である。

[0042]

【数2】

$$\begin{aligned}
 &a_{ik} = a_{ik} - \epsilon_k [(\partial E_j(t) / \partial O_j(t)) (\partial O_j(t) / \\
 &\partial a_{ik}) - a_{ik} + \epsilon_k (S_j(t) - O_j(t)) (\partial O_j(t) / \\
 &\partial a_{ik})]
 \end{aligned}$$

【0044】

【数3】

$$\partial O_j(t) / \partial a_{ik} = \partial \left(\sum_{i=1}^m g_i(t, a_{i1}, a_{i2}, a_{i3}, \dots, a_{iL}) \right) / \partial a_{ik}$$

$$- \partial \lg i(t, a_{i1}, a_{i2}, a_{i3}, \dots, a_{iL}) / \partial a_{ik}$$

【0045】

$$a_{ik} = a_{ik} + \epsilon_k [S_j(t) - O_j(t)] [\partial \lg i(t, a_{i1}, a_{i2}, a_{i3}, \dots, a_{iL})] / \partial a_{ik}$$

【0046】したがって、数4の処理を行なうことによりベクトル成分の推定精度を高め、より正確なベクトル成分を得ることができる。尚、推定誤差 $d_j(t)$ の傾きが正の場合には補正値を負にし、推定誤差 $d_j(t)$ の傾きが負の場合には補正値を正に設定すればよい。以上のようにして各頂点の電流素片のベクトル成分が得られれば、8頂点における電流素片に基づいてベクトルの空間補間処理を行なって各微小点が発生する磁束密度を得、各微小点が発生する磁束密度を積分することにより、各小立方体が発生する磁界を得ることができる。したがって、得られた結果に基づいて分布電流を霧状に表示でき、または矢印によるアロー図で表示できる。

【0047】また、図6の装置に基づく処理は図1または図5の実施例により得られた小立方体（表示立方体に割り当てられた小立方体）のみに基づいて行なえばよいのであるから、臓器等を対象とする場合に、臓器の内部空洞部分等は当初から処理対象に含まれないことになり、処理負荷を低減できる。また、各小立方体の各頂点はかなり高い確率で他の小立方体の頂点を兼ねているのであるから、小立方体の数が増加割合に比して処理対象となる頂点数の増加割合が小さくなり、この点からも処理負荷を低減できる。

【0048】さらに、磁場計測値を得るための測定点数については、一般的な逆問題の解析を行なう場合に未知数の数よりも多い数の測定点が要求されると思われていたのであるが、比較的少ない測定点数で十分なベクトル成分の推定を達成できることを見出した。したがって、測定点数を比較的少なくて済むことに伴なって全体としての処理負荷を低減できることになる。

【0049】この点についてさらに詳細に説明する。従来は臓器等を小立方体の集合として定義することは全く行なわれておらず、したがって、例えば、推定すべき電流素片の数よりも少なくない測定点が必要であった。この結果、電流素片の数が定まつていなければ、十分な安全性を見込んで測定点数を設定していた。具体的には、臓器に流れる電流は時間の経過に伴なって位置および向き、大きさが変化するのであるから、電流素片の数は膨大にならざるを得ない。しかし、この実施例においては、各小立方体の位置が予め固定されているのであるから、測定点に影響を及ぼさない小立方体における電流素

【数4】

$$a_{ik} = a_{ik} + \epsilon_k [S_j(t) - O_j(t)] [\partial \lg i(t, a_{i1}, a_{i2}, a_{i3}, \dots, a_{iL})] / \partial a_{ik}$$

片は0ベクトルに収束してしまうことになる。そして、0ベクトルに収束した電流素片については以後の推定処理が不要になるのであるから、比較的少ない測定点で得られる磁場計測値のみに基づいて高精度のベクトル成分の推定を達成できる。

【0050】

【実施例3】図7はこの発明の生体磁場測定装置の他の実施例を示すブロック図、図8は1つの階層型バーセプトロンに対応する部分の構成を詳細に示す概略図であり、多入力1出力の複数個の階層型バーセプトロン 10^p ($p = 1, 2, \dots, m$) と、階層型バーセプトロン 10^p からの閾値出力 g_{ij} を累積加算するシグマ・ユニット200と、シグマ・ユニット200から出力される累積加算結果 $O_j(t)$ と教師パターンとしての計測値 $S_j(t)$ を入力として両者の差を算出する閾値誤差演算器 3000 と、各階層型バーセプトロン 10^p からの閾値出力 g_{ij} に対応する偏微分値を算出すする偏微分値算出部 $10^p pr$ ($r = 1, 2, \dots, n$) と、各階層型バーセプトロン 10^p の偏微分値算出部 $10^p pr$ からの出力と数値微分法等により算出される偏微分値（偏微分値教師パターン）を入力として両者の差を算出する偏微分値誤差演算器 $300 pr$ と、閾値誤差演算器 300 により算出される差および偏微分値誤差演算器 $300 pr$ により算出される差に基づいて該当する階層型バーセプトロン 10^p に偏微分値の学習を行なわせる偏微分値学習部 $60 p$ と、閾値誤差演算器 300 により算出された累積加算結果 $O_j(t)$ と教師パターンとしての計測値 $S_j(t)$ の差および偏微分値算出部 $10^p pr$ により算出された偏微分値に基づいて階層型バーセプトロン 10^p の入力層における入力を補正する補正部 $12 p$ と、補正部 $12 p$ と偏微分値学習部 $60 p$ を選択するとともに、選択された補正部 $12 p$ または偏微分値学習部 $60 p$ を所定回数（差を十分に小さくできる回数）だけ反復動作させる制御部 400 と、補正部 $12 p$ により補正が所定回数だけ反復されたことを条件として各階層型バーセプトロン 10^p の未知のベクトル成分に対応する入力を未知数量推定結果として出力する情報収集ユニット 5000 を有している。尚、上記各階層型バーセプトロン 10^p は、既知の入力パターンおよび対応する教師パターンを与えて十

分にビオ・サバールの法則に基づく関数の学習を行なつものである。また、階層型バーセプトロン10pはそれぞれ同期的に動作するように制御してもよく、また、非同期的に動作するように制御してもよい。

【0051】また、偏微分間数学習部60pは、例えば、関数値誤差演算器300により算出される差に基づく階層型バーセプトロン10pの学習（例えば、バックプロパゲーション学習）および偏微分値誤差演算器30p rにより算出される差に基づく階層型バーセプトロン10pの学習を交互に反復させることもあり、関数の学習結果を余り損なうことなく偏微分関数の学習を行なえることができる。

【0052】さらに、補正部12pはそれぞれ複数の補正部を有しており、関数値誤差演算器300により算出された差および偏微分値算出部10pkにより算出された差を入力として該当する未知数量を補正する。上記の構成の未知数量推定装置の作用は次のとおりである。各階層型バーセプトロン10pにおいてビオ・サバールの法則に基づく学習が完了しているのであるから、未知のベクトル成分に対応する既知の入力の何れか1つを微小量だけ変化させて出力パターンを得るとともに、偏微分値算出部10pkにより対応する偏微分値を得る。尚、未知のベクトル成分に対応する既知の入力を微小量だけ変化させた場合における偏微分値を数値微分法等により求め算出して偏微分値教師パターンとして与えておく。この状態において制御部40により偏微分間数学習部60pを選択し、選択した偏微分間数学習部60pを所定回数だけ反復動作させることにより再びバックプロパゲーション学習を行い、ビオ・サバールの法則に基づく関数およびこの関数の偏微分間数の演算と等価な処理を達成できるように各階層型バーセプトロン10pを構成するニューロン素子の荷重、閾値を決定する。

【0053】尚、何れかの階層型バーセプトロン10pにより得られた学習結果としての荷重、閾値を他の階層型バーセプトロンの荷重、閾値としてそのまま採用すれば、他の階層型バーセプトロンについては関数の学習および偏微分関数の学習と共に不要にでき、学習所要時間を大幅に短縮できる。以上のようにして必要な学習が完了した後は、偏微分間数学習部60Pに代えて制御部400により補正部12pを選択するとともに情報収集ユニット500を動作させればよく、図6の実施例と同様にベクトル成分を精度よく推定できる。

【0054】

【実施例4】図9はこの発明の生体磁場測定方法のさらに他の実施例を示すブロック図であり、図7および図8の実施例と異なる点は、図7の実施例において階層型バーセプトロン毎に設けられている偏微分値算出部10p rに代えて、1入力のみを微小量だけ変化させる入力変化部15pと、1入力の変化前後における出力を保持する出力保持部16pと、両出力の差を算出する差算出部

17pを設けた点のみである。

【0055】したがって、この実施例の場合には、偏微分演算を行なわなくても、1入力のみの微小変化に対応する出力変化を算出でき、この出力変化が偏微分値に相当するのであるから、上記実施例と同様の作用を達成できる。また、この実施例では偏微分関数の学習が不要になるので、学習所要時間を大幅に短縮できる。

【0056】

【実施例5】図10はこの発明の磁場源測定装置のさらにも他の実施例を示すブロック図であり、1ユニット分のみを示している。複数個の、ビオ・サバールの法則の演算を行なうビオ・サバール演算ユニット11iと、ビオ・サバール演算ユニット11iにおいて推定されている電流素片のベクトル成分を収集して解析結果として出力する電流素片収集ユニット40aと、図1の方法または図5の装置により得られた3次元座標値を基準として修正量 Δx 、 Δy 、 Δz を算出する修正量算出部41iと、算出された修正量 Δx 、 Δy 、 Δz の符号に基づいて、推定されている電流素片のベクトル成分の再配分対象となる隣接頂点を抽出する頂点抽出部42iと、修正量 Δx 、 Δy 、 Δz に基づいて定まる修正ベクトルを正規化する正規化部43iと、正規化された修正ベクトルの各成分の絶対値に基づいて再配分比率を算出する再配分比率算出部44iと、推定されている電流素片のベクトル成分および算出された再配分比率に基づいて抽出された頂点に関して推定されている電流素片のベクトル成分に推定値の再配分を行なう再配分部45iと、再配分部45iにより再配分された再配分値に基づいて該当する電流素片のベクトル成分の推定値を更新する推定値更新部46iと、全ての頂点について修正量 Δx 、 Δy 、 Δz が十分に小さくなるまでビオ・サバール演算ユニット11i、修正量算出部41i、頂点抽出部42i、正規化部43i、再配分比率算出部44i、再配分部45iおよび推定値更新部46iの処理を反復させる反復制御部47iを有している。

【0057】尚、上記推定値更新部46iにおいては、複数の隣接頂点から配分を受ける場合に、各隣接頂点からの再配分比率の加算を行なうのではなく、全ての再配分比率の平均値を算出して現在の値（他の隣接頂点に再配分した残りの割合）に加算することにより新たな推定値を得るようにしている。上記修正量算出部41iは、例えば、ビオ・サバール演算ユニットにより算出された閾数値の偏微分値を算出することにより修正量 Δx 、 Δy 、 Δz を得るものである。

【0058】上記の構成の生体磁場測定装置の作用は次のとおりである。各ビオ・サバール演算ユニットにおいて、

$$g_{ij} = (\mu_0 / 4\pi) \cdot \{ (Y_{j|i} \times p_{xi} - X_{j|i} \times p_{yi}) / R_{j|i}^3 \}$$

50 の演算を行なう。ここで、 μ_0 は透磁率を示し、 i (i

$= 1, 2, \dots, N$) は各小立方体の各頂点における電流素片を、 j ($j = 1, 2, \dots, m$) は測定点をそれぞれ示し、測定点の計測条件を $P_j = (x_j, y_j, z_j)$ 、電流素片の未知の物理量を $U_i = (x_i, y_i, z_i, pxi, pyi)$ とした場合に $X_{j,i} = x_j - x_i, Y_{j,i} = y_j - y_i, Z_{j,i} = z_j - z_i$ であり、 $R_{j,i} = (X_{j,i}^2 + Y_{j,i}^2 + Z_{j,i}^2)^{1/2}$ である。

$$\frac{\partial g_{ij}}{\partial x_i} = \frac{\mu_0}{4\pi} \left\{ \frac{3X_{j,i}(Y_{j,i}px_i - X_{j,i}py_i) + R_{j,i}^2 py_i}{R_{j,i}^5} \right\}$$

【0061】

$$\frac{\partial g_{ij}}{\partial y_i} = \frac{\mu_0}{4\pi} \left\{ \frac{3Y_{j,i}(Y_{j,i}px_i - X_{j,i}py_i) - R_{j,i}^2 pxi}{R_{j,i}^5} \right\}$$

【0062】

【数7】

$$\frac{\partial g_{ij}}{\partial z_i} = \frac{\mu_0}{4\pi} \left\{ \frac{3Z_{j,i}(Y_{j,i}px_i - X_{j,i}py_i)}{R_{j,i}^5} \right\}$$

【0063】

【数8】

$$\frac{\partial g_{ij}}{\partial pxi} = \frac{\mu_0}{4\pi} \frac{Y_{j,i}}{R_{j,i}^3}$$

【0064】

【数9】

$$\frac{\partial g_{ij}}{\partial pyi} = \frac{\mu_0}{4\pi} \frac{X_{j,i}}{R_{j,i}^3}$$

【0065】即ち、数5から数7の偏微分演算と $S_j - O_j$ に基づいて修正量 $\Delta x, \Delta y, \Delta z$ を得ることができる。修正量 $\Delta x, \Delta y, \Delta z$ が得られれば、頂点抽出部42iにより、算出された修正量 $\Delta x, \Delta y, \Delta z$ の符号に基づいて、推定されている電流素片のベクトル成分の再配分対象となる接続頂点を抽出する。具体的には、図11に破線で示すように修正ベクトルが得られるのであるから、二重丸で示される頂点が再配分対象となる隣接頂点として抽出される。そして、正規化部43iにより修正ベクトルを正規化し、正規化された修正ベクトルの各成分の絶対値に基づいて再配分比率算出部44iにより再配分比率を算出し、再配分部45iにより、推定されている電流素片のベクトル成分および頂点抽出部42iにより抽出された頂点に関して推定されている電流素片のベクトル成分に推定値の再配分を行なう。この場合において、各電流素片のベクトル成分は複数の修正ベクトルに基づく再配分が行なわれる可能性があるが、これらを単純に加算すると再配分前の値と再配分後の値とが大幅に異なり、推定の安定性を損なう危険性があるので、推定値更新部46iにおいて、該当する現在の推定値(他の推定値に配分して残りの割合)に対して再配分値の平均(複数の修正ベクトルに基づく再配分比

【0059】したがって、ビオ・サバール演算ユニットにより得られる結果を対応する修正量算出部41に供給すれば、上記演算式を各未知数で偏微分した値が得られる。これらの偏微分値を得るための演算式は数5から数9で与えられる。

【0060】

【数5】

【数6】

$$\frac{\partial g_{ij}}{\partial x_i} = \frac{\mu_0}{4\pi} \left\{ \frac{3X_{j,i}(Y_{j,i}px_i - X_{j,i}py_i) + R_{j,i}^2 py_i}{R_{j,i}^5} \right\}$$

率の平均)を加算することにより新たなベクトル成分推定値を得るようにしている。

【0066】以下、全ての頂点について修正量 $\Delta x, \Delta y, \Delta z$ が十分に小さくなるまで反復制御部47によりビオ・サバール演算ユニット11i、座標値収集ユニット40a、修正量算出部41i、頂点抽出部42i、正規化部43i、再配分比率算出部44i、再配分部45iおよび推定値更新部46iの処理を反復させることにより高精度の電流素片の推定を達成できる。尚、反復制御部47により推定処理を反復させる場合において、各小立方体の各頂点の3次元座標値は固定されているのであるから、上記修正量 $\Delta x, \Delta y, \Delta z$ が直接数5、数6、数7に反映されることはないが、電流素片のベクトル成分は再配分処理により変更されるのであるから、ベクトル成分を通して間接的に反映されることになる。即ち、数5、数6、数7、数8および数9における $X_{j,i}, Y_{j,i}, Z_{j,i}, R_{j,i}$ は推定開始当初から推定終了まで変化せず、 pxi, pyi のみが変化し、最終的に高精度に推定された pxi, pyi を得ることができるのである。この結果、例えば図12(A)に示すように、互にキャンセルし合う電流素片が互に近接する位置に割り当てられていても、再配分処理を行なうことにより図12(B)に示すように推定が行なわれ、電流が存在しない位置に互にキャンセルし合う電流が残留するという不都合を確実に解消できる。尚、図12中、黒丸が処理対象頂点を、白丸が隣接する頂点を示している。

【0067】図14から図18は1チャネルのマグネットメータを用いて3cm間隔、 6×6 点で計測した心磁図を心電図を用いて同期加算して得た磁界分布図に基づいてQ波近傍時刻の磁場源推定結果を示す図であり、医学的に確認されている心臓の体積電流に高精度に近似できる推定結果が得られていることが分る。尚、図13はMRI画像に基づいて得られた深さが6cmの頂点情報であり、図14から図18はそれぞれR波出現前3.5msec、3.3msec、3.0msec、2.5msec、2.0msecの時刻に対応

する推定結果であり、大きい黒丸が心臓の壁を示しているとともに、黒丸を起点とする線分で電流素片を示している。

【0068】尚、この実施例において、各ビオ・サバール演算ユニットに代えて階層型パーセプトロンを採用することができる。

【0069】

【実施例7】図19はこの発明の生体磁場測定結果表示方法の一実施例を説明するフローチャートであり、ステップSP1において、生体断層像に対応する平面内における、所定の時点における電流素片の位置および大きさ(興奮電流の絶対値)が得られるまで待ち、ステップSP2において複数の電流素片のそれぞれの大きさに対応する直径の円を割り当て、ステップSP3において生体断層像を表示し、ステップSP4において、割り当てられた円を対応箇所に生体断層像とオーバーラップした状態で表示し、ステップSP5において興奮電流表示の終了が指示されたか否かを判別し、終了が指示されていない場合には、ステップSP6において異なる時点における電流素片の位置および大きさが得られるまで待ってから再びステップSP2の処理を行なう。逆に、ステップSP5において終了が指示された場合にはそのまま一連の処理を終了する。但し、ステップSP2における円の割り当てについていえば、電流素片の大きさに正確に対応する直径の円を割り当てるようにしてよいが、電流素片の大きさを複数段階に区分し、各区分に対応して段階的に変化するように円の直径を割り当ててもよい。

【0070】

【実施例8】図20はこの発明の生体磁場測定結果表示方法の他の実施例を説明するフローチャートであり、ステップSP1において、生体断層像に対応する平面内における臓器等の存在箇所が検出されるまで待ち、ステップSP2において臓器等の存在箇所に對応して所定の直径の通常の円を割り当て、ステップSP3において上記平面内における、所定の時点における電流素片の位置および大きさが得られるまで待ち、ステップSP4において、該当する円に代えて複数の電流素片のそれぞれの大きさに對応する直径の強調表示円を割り当て、ステップSP5において生体断層像を表示し、ステップSP6において、割り当てられた円を対応箇所に生体断層像とオーバーラップした状態で表示し、ステップSP7において興奮電流表示の終了が指示されたか否かを判別し、終了が指示されていない場合には、ステップSP8において異なる時点における電流素片の位置および大きさが得られるまで待ってから再びステップSP4の処理を行なう。逆に、ステップSP7において終了が指示された場合にはそのまま一連の処理を終了する。

【0071】図21はこの実施例による興奮電流の表示例を示す図であり、著しく高い視認性を發揮できていることが分かる。また、興奮電流が存在していない箇所にお

いても識器等に対応して通常の円が表示されているとともに、円同士の間にはかなりの間隔が存在し、この間隔を通して断層像を簡単に確認できる。特に、時系列的に興奮電流を表示する場合には、例えば最大の興奮電流が変化する状態を簡単に把握できることになる。

【0072】

【実施例9】図22はこの発明の生体磁場測定結果表示方法のさらに他の実施例を説明するフローチャートであり、ステップSP1において所定の時点における電流素片の位置および大きさが得られるまで待ち、ステップSP2において複数の電流素片のそれぞれの大きさに対応する直径の球を割り当て、ステップSP3において生体構造参照像を3次元的に半透明表示し、ステップSP4において、割り当てられた球を対応箇所に生体構造参照像とオーバーラップした状態で表示し、ステップSP5において興奮電流表示の終了が指示されたか否かを判別し、終了が指示されていない場合には、ステップSP6において異なる時点における電流素片の位置および大きさが得られるまで待ってから再びステップSP2の処理を行なう。逆に、ステップSP5において終了が指示された場合にはそのまま一連の処理を終了する。

【0073】したがって、この実施例の場合には、3次元的な生体構造参照像に對応付けて電流素片の大きさに對応する直径の球を表示でき、時系列的に球の表示を行なうことにより興奮電流の3次元的伝播方向を簡単に把握できることになる。

【0074】

【実施例10】図23はこの発明の生体磁場測定結果表示装置の一実施例を示すブロック図であり、電流素片解析結果を保持する解析結果保持部600と、電流素片の大きさに對応する直径の円を割り当てる円割り当てる部700と、生体断層像を表示する断層像表示部800と、断層像とオーバーラップさせた状態で割り当てられた直径の円を表示する円表示部900とを有している。

【0075】したがって、生体断層像の表示とオーバーラップさせて電流素片の大きさに對応する円を表示でき、興奮電流の視認性を著しく高めることができる。そして、時系列的に解析結果に基づいて円のオーバーラップ表示を行なうことにより興奮電流の伝播方向を簡単に把握できる。尚、上記実施例7～10において、例えば、生体像の視認性の多少の低下を許容できる場合には、円に代えて正方形、球に代えて立方体を表示することが可能であるほか、この発明の要旨を変更しない範囲内において種々の設計変更を施すことが可能である。

【0076】

【発明の効果】以上のように請求項1の発明は、所定間隔毎の断層像しか得られていないても、補間演算を行なうことにより全空間に對応して立体像データを得、しかも区分された小立体領域に含まれる立体像データの数に基づいて小立体領域を2値化することにより単純化され

た立体像を得ることができ、ひいては、可視的に表示した場合に、臓器等に相当する箇所、空間に相当する箇所を簡単に認識できるという特有の効果を奏する。

【0077】請求項2の発明も、所定間隔毎の断層像しか得られていくとも、補間演算を行なうことにより全空間に対応して立体像データを得、しかも区分された小立体領域に含まれる立体像データの数に基づいて小立体領域を2値化することにより単純化された立体像を得ることができ、ひいては、可視的に表示した場合に、臓器等に相当する箇所、空間に相当する箇所を簡単に認識できるという特有の効果を奏する。

【0078】請求項3の発明は、複数のビオ・サバールの法則の演算結果の累積加算値が磁場計測値と高精度に近似されるまで補正を行なうことにより、各小立体領域の頂点における磁場源情報を得ることができ、全体として処理負荷を大幅に低減できるという特有の効果を奏する。請求項4の発明は、互に近接する状態で割り当てられた、大きさが互に等しくかつ向きが互に逆の磁場源ベクトルが存在していても、これらを確実に補正でき、一層高精度に推定された磁場源情報を得ることができるとともに、隣接する頂点間で再配分を行なうことにより推定を行なうのであるから、推定対象となる磁場源情報の数に見合って從来必要とされていた測定点数よりも少ない測定点に基づいて高精度の磁場源推定を達成できるという特有の効果を奏す。

【0079】請求項5の発明も、複数のビオ・サバールの法則の演算結果の累積加算値が磁場計測値と高精度に近似されるまで補正を行なうことにより、各小立体領域の頂点における磁場源情報を得ることができ、全体として処理負荷を大幅に低減できるという特有の効果を奏する。請求項6の発明も、互に近接する状態で割り当てられた、大きさが互に等しくかつ向きが互に逆の磁場源ベクトルが存在していても、これらを確実に補正でき、一層高精度に推定された磁場源情報を得ることができるとともに、隣接する頂点間で再配分を行なうことにより推定を行なうのであるから、推定対象となる磁場源情報の数に見合って從来必要とされていた測定点数よりも少ない測定点に基づいて高精度の磁場源推定を達成できるという特有の効果を奏す。

【0080】請求項7の発明は、生体構造参照像を表示するとともに、生体構造参照像の該当位置に設定されたサイズの単位图形を表示するのであるから、矢印の方向と長さで物理量計測結果を表示する場合と比較して、例えば、最大の生体物理量計測結果の分布状態を簡単に認識できとともに、生体物理量計測結果を動的に表示することにより、例えば、最大の生体物理量計測結果の分布状態の時間的変動を簡単に認識できるという特有の効果を奏す。

【0081】請求項8の発明は、請求項7の効果に加え、単位图形が円であるから、単位图形同士の隙間をか

なり大きくでき、背景となる生体構造参照像の把握が容易になるという特有の効果を奏する。請求項9の発明は、生体構造参照像を表示するとともに、生体構造参照像の該当位置に設定されたサイズの単位图形を表示するのであるから、矢印の方向と長さで物理量計測結果を表示する場合と比較して、例えば、最大の生体物理量計測結果の分布状態を簡単に認識できとともに、生体物理量計測結果を表示することにより、例えば、最大の生体物理量計測結果の分布状態の時間的変動を簡単に認識できるという特有の効果を奏す。

【0082】請求項10の発明は、請求項9の効果に加え、単位图形が円であるから、単位图形同士の隙間をかなり大きくでき、背景となる生体構造参照像の把握が容易になるという特有の効果を奏する。

【図面の簡単な説明】

【0083】

【図1】この発明の断層像処理方法の一実例を説明するフローチャートである。

【0084】

【図2】断層像の一例を示す概略図である。

【0085】

【図3】表示立方体と非表示立方体との割り当て状態を概略的に示す平面図である。

【0086】

【図4】図3に対応する斜視図である。

【0087】

【図5】この発明の断層像処理装置の一実例を示すブロック図である。

【0088】

【図6】この発明の生体磁場測定装置の一実例を示すブロック図である。

【0089】

【図7】この発明の生体磁場測定装置の他の実例を示すブロック図である。

【0090】

【図8】1つの階層型バーセプトロンに対応する部分の構成を詳細に示す概略図である。

【0091】

【図9】この発明の生体磁場測定方法のさらに他の実施例を示すブロック図である。

【0092】

【図10】この発明の磁場源測定装置のさらに他の実施例を示すブロック図である。

【0093】

【図11】推定されている電流素片のベクトル成分の再配分対象となる隣接頂点を抽出する処理を説明する概略図である。

【0094】

【図12】再配分による電流素片の推定処理を説明する概略図である。

【0095】

【図13】MR1画像に基づいて得られた深さが6cmの頂点情報を示す図である。

【0096】

【図14】R波出現前3.5msecに対応する推定結果を示す図である。

【0097】

【図15】R波出現前3.3msecに対応する推定結果を示す図である。

【0098】

【図16】R波出現前3.0msecに対応する推定結果を示す図である。

【0099】

【図17】R波出現前2.5msecに対応する推定結果を示す図である。

【0100】

【図18】R波出現前2.0msecに対応する推定結果を示す図である。

【0101】

【図19】この発明の生体磁場測定結果表示方法の一実施例を説明するフローチャートである。

【0102】

【図20】この発明の生体磁場測定結果表示方法の他の実施例を説明するフローチャートである。

【0103】

【図21】図20の実施例による興奮電流の表示例を示す図である。

【0104】

【図22】この発明の生体磁場測定結果表示方法のさらに他の実施例を説明するフローチャートである。

【0105】

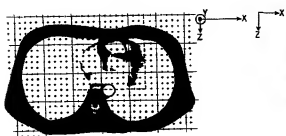
【図23】この発明の生体磁場測定結果表示装置の一実施例としての興奮電流表示装置を示すブロック図である。

【0106】

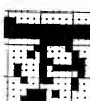
【符号の説明】

10	3 断層像捕間部	7 立方体割り当て部	8 画素数計数部
9	判別部	10 表示立方体割当部	20, 20
0	シグマ・ユニット		
30	3, 000 誤差演算器	41 i 修正量算出部	
4	421 頂点抽出部		
431	正規化部	441 再配分比率算出部	4
51	再配分部		
461	推定値更新部	40, 500 情報収集ユニット	
20	101, 102, ..., 10m 階層型バーセプトロン		
111, 112, ..., 11m	ビオ・サバール演算ユニット		
111a, 112a, ..., 11ma, 121, 122, ..., 12m	補正部		
700	円割り当て部	800 断層像表示部	
900	円表示部		

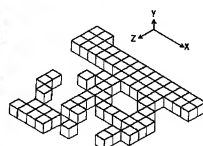
【図2】



【図3】

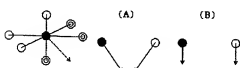


【図4】

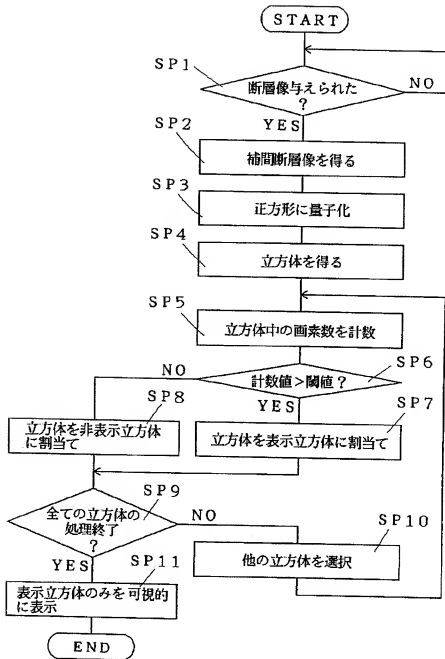


【図11】

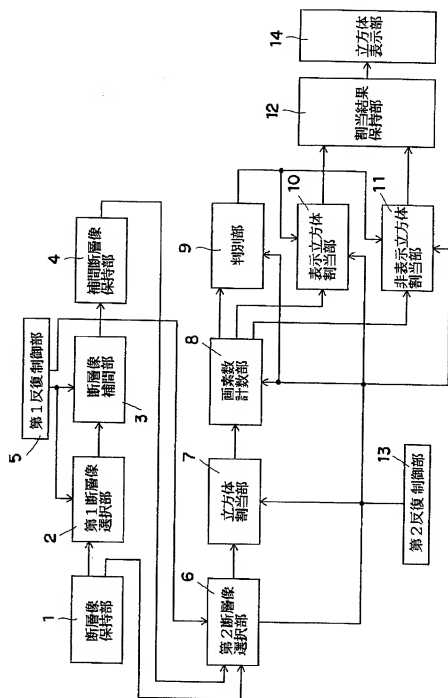
【図12】



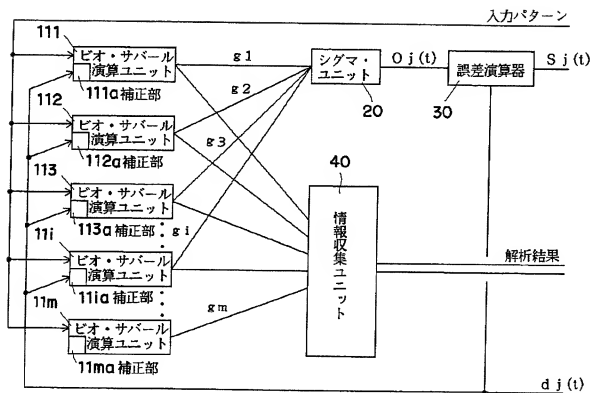
【図1】



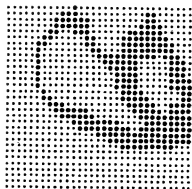
【図5】



【図6】



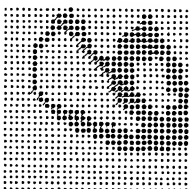
【図13】



【図14】



【図15】



【図7】

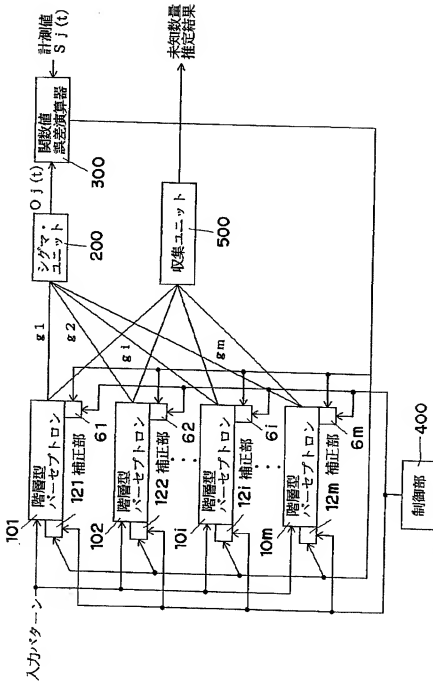
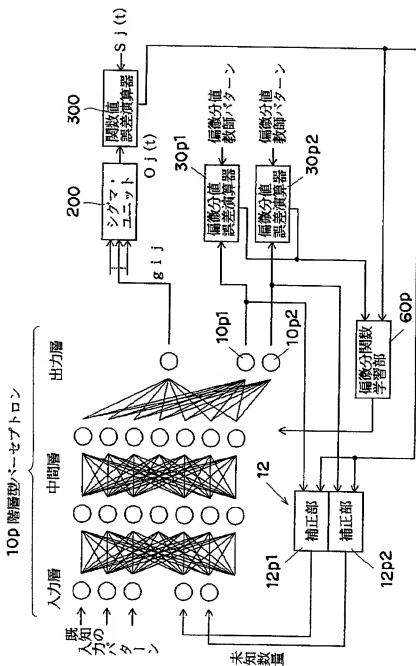
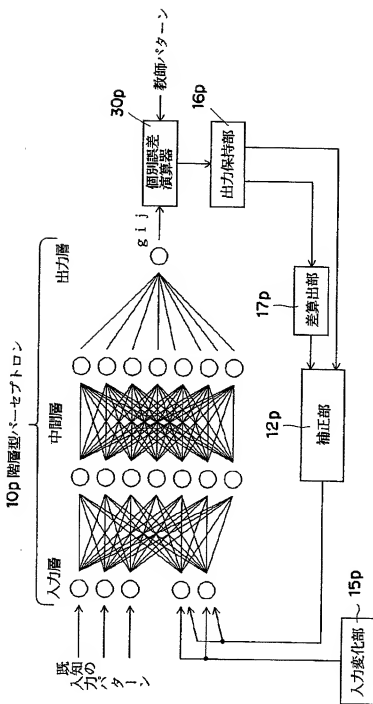


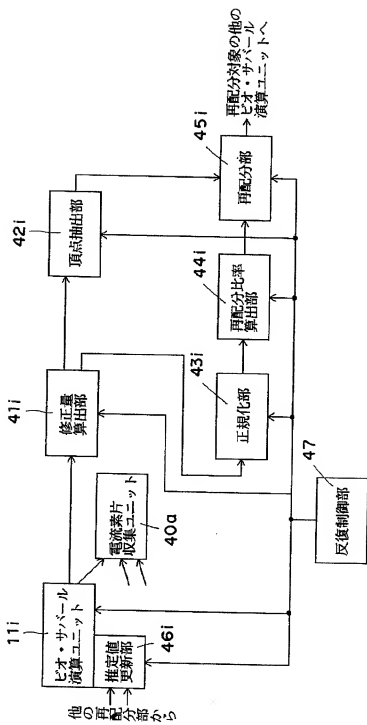
[圖 8]



【図9】



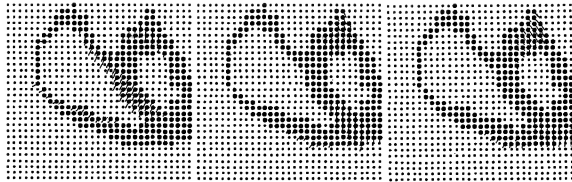
【図10】



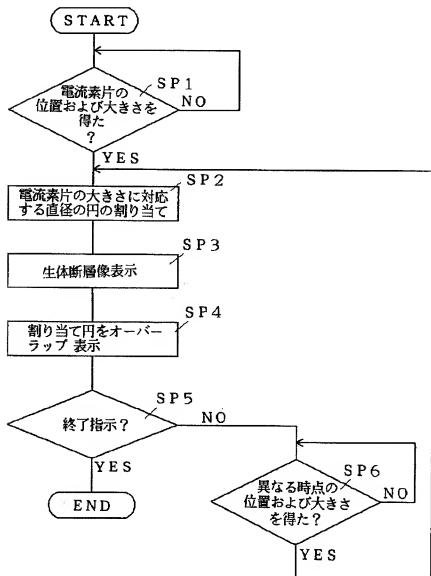
【図16】

【図17】

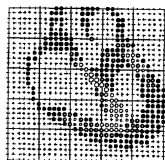
【図18】



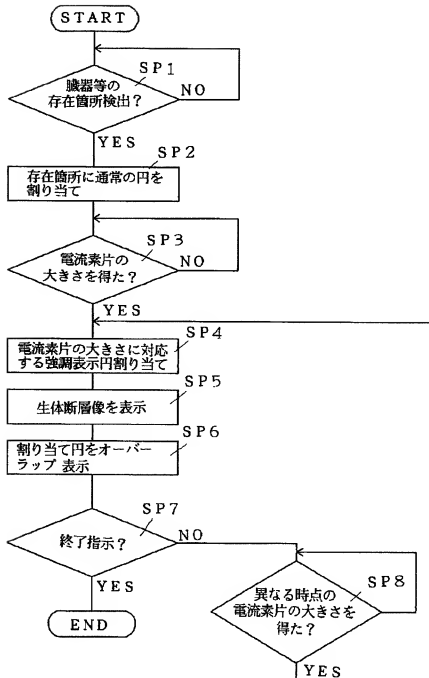
【図19】



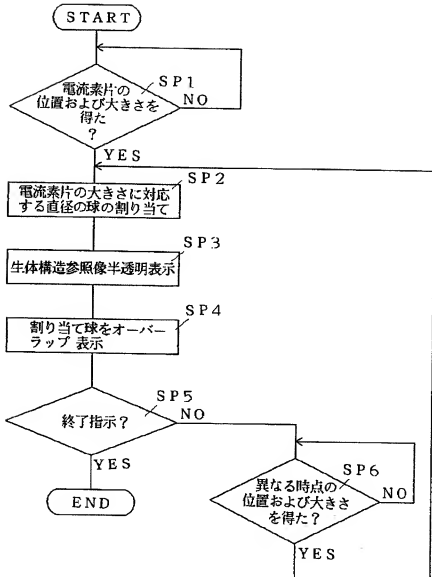
【図21】



【図20】



【図22】



【図23】

